Model Size and Humidity Effects on Selected Calibration Parameters for the 16-ft Transonic Wind Tunnel at AEDC

Ernest J. Lucas
ARO, Inc.

November 1981

Final Report for Period October 1, 1978 — December 31, 1980

ARNOLD ENGINEERING DEVELOPMENT CENTER
ARNOLD AIR FORCE STATION, TENNESSEE
AIR FORCE SYSTEMS COMMAND
UNITED STATES AIR FORCE

This report has been reviewed by the Office of Public Affairs (PA) and is releasable to the National Technical Information Service (NTIS). At NTIS, it will be available to the general public, including foreign nations.

APPROVAL STATEMENT

This report has been reviewed and approved.

KEITH L. KUSHMAN
Directorate of Technology
Deputy for Operations

Approved for publication:

FOR THE COMMANDER

MARION L. LASTER
Director of Technology
Deputy for Operations

SECURITY CLASSIFICATION OF THIS PAGE *(When Data Entered)*

REPORT DOCUMENTATION PAGE	READ INSTRUCTIONS BEFORE COMPLETING FORM

1 REPORT NUMBER	2 GOVT ACCESSION NO	3 RECIPIENT'S CATALOG NUMBER
AEDC-TR-81-17		

4 TITLE *(and Subtitle)*	5 TYPE OF REPORT & PERIOD COVERED
MODEL SIZE AND HUMIDITY EFFECTS ON SELECTED CALIBRATION PARAMETERS FOR THE 16-FT TRANSONIC WIND TUNNEL AT AEDC	Final Report – Oct. 1, 1978 – Dec. 31, 1980
	6 PERFORMING ORG. REPORT NUMBER

7 AUTHOR(s)	8 CONTRACT OR GRANT NUMBER(s)
Ernest J. Lucas, ARO, Inc., AEDC Group (a Sverdrup Corporation Company)	

9. PERFORMING ORGANIZATION NAME AND ADDRESS	10 PROGRAM ELEMENT, PROJECT, TASK AREA & WORK UNIT NUMBERS
Arnold Engineering Development Center/DOT Air Force Systems Command Arnold Air Force Station, TN 37389	Program Element 65807F

11 CONTROLLING OFFICE NAME AND ADDRESS	12 REPORT DATE
Arnold Engineering Development Center/DOS Air Force Systems Command Arnold Air Force Station, TN 37389	November 1981
	13 NUMBER OF PAGES
	47

14 MONITORING AGENCY NAME & ADDRESS*(if different from Controlling Office)*	15 SECURITY CLASS *(of this report)*
	UNCLASSIFIED
	15a DECLASSIFICATION/DOWNGRADING SCHEDULE N/A

16 DISTRIBUTION STATEMENT *(of this Report)*

Approved for public release; distribution unlimited.

17 DISTRIBUTION STATEMENT *(of the abstract entered in Block 20, if different from Report)*

18. SUPPLEMENTARY NOTES

Available in Defense Technical Information Center (DTIC).

19. KEY WORDS *(Continue on reverse side if necessary and identify by block number)*

wind tunnel tests	dew point
Reynolds number	free stream
test facilities	wind tunnel models
calibration	

20 ABSTRACT *(Continue on reverse side if necessary and identify by block number)*

Analyses of wind tunnel wall surface pressure data and model force data from tests conducted in the Propulsion Wind Tunnel (16T) with 1/9- and 1/4-scale fighter models were conducted to determine the effect of model size, location, and attitude, and tunnel flow humidity and Reynolds number on the test section calibration. The tests were conducted at Mach numbers from 0.6 to 1.4 at Reynolds numbers from 1.8×10^6/ft to 4.8×10^6/ft,

20. ABSTRACT (Continued)

depending on model structural limits and Mach number. The model influence was localized and did not affect the set conditions of the flow entering the test section. The currently used Reynolds number calibration is valid within the uncertainty of the instrumentation installed in the Tunnel 16T system. Analysis of the data indicates that the test section dewpoint should be below the free-stream static temperature to prevent humidity effects on model force data.

PREFACE

The work reported herein was conducted by the Arnold Engineering Development Center (AEDC), Air Force Systems Command (AFSC), under Program Element 65807F at the request of AEDC Directorate of Technology (DOT). The DOT project managers were Elton Thompson, Alex Money, and Keith Kushman; the ARO, Inc., project engineer was Ernest J. Lucas. The results were obtained by ARO, Inc., AEDC Group (a Sverdrup Corporation Company), operating contractor for the AEDC, AFSC, Arnold Air Force Station, TN. The analyses and test were conducted during the period from October 1, 1979 through April 30, 1981, under AEDC Project Number D201PW. The manuscript was submitted for publication on June 3, 1981.

Mr. Ernest J. Lucas is currently employed by Calspan Field Services, Inc./AEDC Division.

CONTENTS

ILLUSTRATIONS

TABLES

1.0 INTRODUCTION

The program reported herein was conducted to determine the validity of the currently accepted calibration techniques by obtaining independent static pressure data within the AEDC Propulsion Wind Tunnel (16T) nozzle and test section while varying the model size, axial location, Mach number, Reynolds number, and free-stream humidity. A 1/9- and 1/4-scale aerodynamic model of a single engine fighter aircraft was selected for the investigation. A summary of the test conditions investigated under Project No. P41T-F6 is presented in Table 1.

2.0 TEST FACILITY

The AEDC Propulsion Wind Tunnel (16T) is a variable density, continuous-flow tunnel capable of operating at Mach numbers from 0.2 to 1.5 and stagnation pressures from 120 to 4,000 psfa. The maximum attainable Mach numbers can vary slightly, depending upon the tunnel pressure ratio requirements with a particular test installation. The maximum stagnation pressure attainable is a function of Mach number and available electrical power. The tunnel stagnation temperature can be varied from about 80 to 160°F, depending upon the cooling water temperature. The tunnel is equipped with a scavenging system to remove combustion products when rocket motors or turbo-engines are tested. The test section is 16-ft square by 40 ft long and enclosed by 60-deg inclined-hole perforated walls of six-percent porosity. The general arrangement of the test section and the test article location is shown in Fig. 1. Additional information about the tunnel, its capabilities, and operating characteristics is presented in Ref. 1.

3.0 PROCEDURE

3.1 DATA ACQUISITION

The model aerodynamic loadings were obtained from internally mounted six-component balances, and the model internal cavity pressures were recorded with a model-mounted pressure transducer system. The tunnel test section top and bottom wall and nozzle wall static pressures were recorded on the standard tunnel 16T pressure measuring system. Free-stream static conditions were obtained through a calibration algorithm from measurements of the tunnel total pressure, total temperature, and plenum chamber pressure. The current calibration data and algorithm development are presented in Ref. 2. All data were recorded concurrently after pressure and force measurements stabilized following each model repositioning or tunnel condition change.

3.2 DATA REDUCTION

The facility standard force and moment data reduction procedure was used to reduce the balance data with corrections applied for weight tares and cavity pressure. The force data were nondimensionalized to coefficient form, based on the model wing planform area (S) and appropriate reference lengths (b, $\bar{c}$).

The wind tunnel wall static pressures (Figs. 1 and 2) were reduced to coefficient form based on the calculated free-stream static and dynamic pressures. The local wall static pressures were also used to calculate various pressure ratios and Mach number functions which were used in the analysis to determine the influence of the models and flow humidity on the set conditions in the test section.

3.3 TEST SECTION FLOW ANGULARITY

The test section centerline flow angularity was determined for both the 1/9- and 1/4-scale sting supported models (Fig. 3) by obtaining aerodynamic lift data on the models upright and inverted over an angle-of-attack range of -4 to 4 deg. The flow angles were determined at Mach numbers from 0.6 to 1.4, and the results are presented in Fig. 4 for test conditions shown in Table 1. Some of the differences shown are caused by differences in test conditions since the data were acquired at matched characteristic Reynolds numbers. The flow angularity defined in this effort is within the angle measurement uncertainty of ±0.1 deg.

As generally accepted, flow angularity corrections were applied over the total model angle-of-attack range of -4 to 8 deg. For both models on the sting support system at the center of rotation selected, the model remains in the vicinity of the tunnel centerline throughout the model pitch attitude excursion.

3.4 FLOW MEDIUM MOISTURE CONTENT VARIATION

The presence of water vapor in the airflow of wind tunnels can influence test data, especially in large transonic or supersonic test facilities. To investigate this phenomenon and the interrelation with model size on local test conditions, steam was added to the tunnel flow downstream of the test section. The moisture then had sufficient time to fully mix through the compressor and back sections of the continuous-flow tunnel before entering the stilling chamber where the dewpoint temperature was measured. The dewpoint temperature measurement was then adjusted to the test section conditions for comparison to the free-stream static temperature.

Data were acquired with both the 1/9- and 1/4-scale models at 6-deg angle of attack while the moisture in the tunnel flow was being increased by steam addition or decreased by the Tunnel 16T desiccant drier. Model angle-of-attack excursions were also made at the limits of the moisture addition and drying cycles to provide data for determining the moisture content effect on the model aerodynamic loads at Mach numbers 0.6, 0.9, and 1.2.

3.5 DATA UNCERTAINTY

Uncertainties (combinations of systematic and random errors) of the basic tunnel parameters, shown in Fig. 5, were estimated from repeat calibrations of the instrumentation and from the repeatability and uniformity of the test section flow during tunnel calibration. Uncertainties in the instrumentation systems were estimated from repeat calibration of the systems against secondary standards whose uncertainties are traceable to the National Bureau of Standards calibration equipment. The tunnel parameter and instrument uncertainties are combined using the Taylor series method of error propagation described in Ref. 3 to determine the uncertainties of the reduced parameters. These uncertainties, for a 95-percent confidence level, are shown in Table 2.

4.0 RESULTS AND DISCUSSION

4.1 MODEL SIZE, ATTITUDE, AND LOCATION EFFECTS ON WIND TUNNEL CALIBRATION

Historically, the PWT wind tunnels have been calibrated based on the average of either the tunnel centerline static pressures obtained from a pipe supported along the test section centerline, or from static pressures along the centerline of the top and bottom walls, as discussed in Refs. 2 and 4. Current porous wall transonic wind tunnel calibration techniques do not include correction for possible changes in the calibration with pressure drop through the wall as a result of installation or attitude of the model being tested. The assumption is that free-stream conditions are a unique function of the stilling chamber and plenum pressure for a given test section configuration. For very small models this is a valid assumption. However, for larger models, blockage effects or tunnel boundary-layer and model shock interactions could produce a change in the wall pressure drop and thus a different free-stream static pressure for a given plenum pressure. Test section wall static pressures and a ring of static pressures upstream of the test section (Tunnel Station -4 ft) were measured to determine if differences in the free-stream flow existed when a typical model and a model that approaches the limits of length and span for vehicle performance are tested in Tunnel 16T. Other calibration parameters such as Reynolds number, wall angle, and stream moisture content were also evaluated with respect to the effect on the calibration and model forces.

7

The local effect of model size on the test section condition is illustrated in Fig. 6 where the differences in the average of the top and bottom test section wall pressures obtained with the 1/4- and 1/9-scale model installations are presented for each orifice location along the test section wall. The theoretical pressure distribution presented for Mach number 0.9 was obtained by modeling the 1/9- and 1/4-scale configurations as an equivalent body of revolution and assuming a linear wall characteristic boundary condition. The agreement between the measured and calculated pressure distribution is quite good, illustrating that the measured wall pressure distribution is indicative of the presence of the model. Although measurable effect of model size on the local wall pressure is evident as expected at subsonic Mach numbers, the effect does not extend upstream of the test section. It is interesting to note at subsonic speeds that if the top and bottom wall pressures are averaged over the test section length, the model size influence on the average wall pressure is negligible.

The shock systems for the two models do not coincide because of the axial difference in model location and length; thus, there are large variations in the local wall pressure coefficients that are isolated downstream of the initial 1/4-scale shock intersection with the tunnel wall. The flow field at the entrance to the test section is the same for the two model sizes at all Mach numbers investigated.

As would be expected, the effect of model attitude on the local wall pressures is larger for the 1/4-scale model, as shown in Fig. 7. However, when the top and bottom wall pressures at a given station are averaged, the average value at any station is near the undisturbed free-stream value ($C_p = 0$). More importantly, the model attitude does not influence the flow entering the test section at any Mach number investigated.

The effect of moving the 1/9-scale model forward in the test section is illustrated in the differential wall pressure data presented in Fig. 8. The changes in the wall pressure data are less than those for model size influence. The only significant changes occur in the model shock intersection region of the walls. Thus, model location effects are isolated downstream of the test section entrance.

A more representative measurement of the undisturbed average pressure of the flow approaching the test section may be obtained from multiple measurements at a fixed tunnel station upstream of the removable test section. To investigate that hypothesis, pressure orifices were installed at a tunnel station 4 ft upstream (TS-4) of the test section entrance. The wall pressure distribution at Tunnel Station -4, presented in Fig. 9, indicates that the local pressures are higher than the calculated free-stream static pressure, but, as expected, no model influence is evident. The positive pressure coefficient values indicate lower local Mach numbers upstream of the test section. Such a condition is consistent with the normal flow

development which results from boundary-layer growth on the tunnel walls. An unexpected difference was observed in the tunnel sidewall pressure data at Mach number 1.1 (Fig. 9b) that was not evident on the top and bottom walls or at other Mach numbers. The influence of the model should be downstream of the model if supersonic flow exists. However, since only the sidewalls are affected, the discrepancy appears to be a local sidewall related disturbance, which is associated with the tunnel sidewall movement. The local disturbance on the sidewalls at Mach number 1.1 occurred intermittently for both models. The reason for the disturbances has not been determined.

The overall average influence of model size on the Tunnel Station -4 parameters is illustrated in Fig. 10, with the east and west wall pressures deleted for the Mach number 1.1 data. No measurable dependence of test article configuration is evident at any of the conditions investigated since the calculated Mach number deviations are well within the quoted uncertainty.

4.2 REYNOLDS NUMBER EFFECT

Analysis of test data which indicated large Reynolds number effects (Ref. 5) revealed large effects of Reynolds number on the tunnel calibration. Tunnel 16T was recalibrated to include the effects of Reynolds number on the calibration parameters. The results are reported in Ref. 2.

The current program was conducted with the Reynolds number correction included in the tunnel calibration algorithm. The influence of changing the free-stream Reynolds number on the test section wall pressures with the 1/9-scale model is shown in Fig. 11. At Mach number 0.6, changing the free-stream Reynolds number produced gradients in the wall static pressure distribution that are not totally corrected by the current calibration. In general, however, the local deviations in pressure coefficient from the calculated free-stream conditions are within the uncertainty (Table 2) of the measurements which correspond to approximately ± 0.001 in Mach number.

The average of all the test section wall orifice measurements (M_W) at subsonic Mach numbers and those ahead of the model shock-wall intersection at supersonic speeds should be proportional to the set calibration Mach number (M_∞). The Mach number differences, ($M_\infty - M_W$) and ($M_W - MN$), for the two models are presented as a function of free-stream Reynolds number in Fig. 12. Both parameters are essentially insensitive to Reynolds number within the measurement uncertainty. The current calibration differential ($M_\infty - M_W$) variation is within ± 0.001; however, a second-order algorithm correction could possibly reduce that variation further, especially at Mach number 0.6. The term ($M_W - MN$) is based

on measured local pressures and the tunnel stilling chamber total pressure; thus, it is independent of the tunnel calibration. The Mach number calculated from the Tunnel Station -4 pressures is not equal to the calibrated test section conditions because of the influence of the tunnel boundary layer and porous walls. At Mach numbers 1.1 and 1.2 (Fig. 12c), $M_\infty - M_W$ is significantly different from zero. This is caused by local disturbances in the upstream end of the test section, as shown in Fig. 13. The disturbances are the same for both models, indicating an inherent tunnel phenomenon at Mach numbers 1.1 and 1.2 that was not measured at other Mach numbers. The pressure downstream of station 6 is nearer the calibration (i.e., $C_p = 0$) at Mach number 1.2 but still low at Mach number 1.1. The tunnel calibration (Ref. 3) is an average of centerline pressure measurements from station 6 to 18 ft. Test articles should be installed downstream of station 6 when testing is to be conducted at Mach numbers 1.1 or 1.2. All measured Reynolds number effects on the current tunnel calibration are within the measurement uncertainty. The independent measurements at Tunnel Station -4 indicate essentially the same sensitivity to Reynolds number as the current calibration but offer no significant improvement over the existing calibration procedure and algorithm.

4.3 WALL ANGLE INFLUENCE

The Tunnel 16T test section sidewalls can be converged or diverged (Refs. 2 and 4) and are used either in the zero wall angle mode (walls parallel) or with a wall angle schedule as a function of Mach number to provide the best wall wave cancellation characteristics (Ref. 6). Both wall angle schedules were investigated with each scale model. Although the test section wall pressure data in the vicinity of the models indicated a model size dependence (Fig. 6b), the first six orifices on the top and bottom walls were essentially unaffected by model size or placement.

The average of these pressures, although not the free-stream value, does provide an indication of the wall angle effect on the flow field entering the test section. The test section sidewalls are set to zero for all subsonic operations. Model size did not alter the effects of wall angle as shown in Fig. 14. The differences with wall angle at supersonic Mach numbers, although measurable, are within the measurement uncertainty and thus are insignificant.

Differences in the average Tunnel Station -4 wall pressure coefficient between the optimum and zero wall angle settings are presented in Fig. 15. The Station -4 pressures are essentially independent of the test section wall angle at supersonic Mach numbers as would be expected , except for the previously discussed Mach number 1.1 data. The individual pressure coefficients are presented in Fig. 16 for Mach numbers 1.1 and 1.2. Since supersonic flow exists at Tunnel Station -4 at Mach number 1.1, the difference in pressure

coefficient between two model scales indicates some local interference or calibration problem at Mach number 1.1. This difference is not evident at Mach number 1.2 (Fig. 16b).

4.4 INFLUENCE OF MOISTURE CONTENT ON TUNNEL CALIBRATION

The quantity of water vapor in the tunnel flow and the free-stream static temperature relative to the dewpoint temperature in the test section flow can produce changes in the test environment. These effects are not readily evident since the tunnel test section conditions are established based on measurements of the pressure in the stilling chamber and the plenum area and not with moisture as a parameter. Thus, any influence of moisture on the calibration is not obvious.

The effect of variations in tunnel humidity as represented by changes in the dewpoint temperature on typical average Mach numbers at Tunnel Station -4 is shown in Fig. 17. At subsonic speeds there was no effect of changing the flow moisture content over the range investigated for either model. However, varying the moisture content of the flow at Mach number 1.2 produced significant changes in the Tunnel Station -4 Mach numbers, although the calibration algorithm indicated the test section Mach number to be correct. These data at Tunnel Station -4 indicate it is possible to operate at Mach number 1.2 with approximately 20° of supercooling, based on the dewpoint temperature readings for this test as shown in Fig. 17b. The currently established humidity limits for Tunnel 16T are to operate at dewpoint temperature below the free-stream static temperature at subsonic speeds and to maintain the specific humidity below 0.0015 at supersonic test conditions since it is not possible with typical stagnation temperatures to achieve dewpoint temperatures lower than the dry bulb temperature at Mach numbers above 1.2.

The effect of humidity at Tunnel Station -4 was further analyzed by calculating differential pressure coefficients from the humidity variations on both models at Mach number 1.2, as shown in Fig. 18. The humidity influence is isolated along the tunnel vertical centerline, away from the diverging nozzle sidewalls. This effect is lessened by the time the flow enters the test section, as observed by comparing the $(T_{\infty} - T_{DP})$ at which the data become invariant (Figs. 17b and 19). The data in Fig. 19 are an average of the data from the first six orifices (TS 1 to 6 ft) on the test section top and bottom wall centerline. These test section data indicate the tunnel calibration at Mach number 1.2 is correct at dewpoint temperatures 30° above the static temperature. However, the influence of humidity on the model aerodynamics must also be assessed.

4.5 MODEL MEASUREMENTS

The effects of changing moisture content $(T_\infty - T_{DP})$ of the test section flow on the model aerodynamic loads with the model at 6-deg angle of attack are illustrated in Fig. 20. The differences presented were obtained by subtracting the coefficients at each humidity condition from the driest condition obtained at each Mach number. Thus, the differences in each coefficient must indicate several consecutive zero values to indicate an insensitivity to further humidity decrease.

The tunnel moisture content at $M_\infty = 0.6$ could not be elevated to a value such that the dewpoint temperature was above the static temperature. As a result there was no apparent effect of moisture content on the 1/4-scale model data at Mach number 0.6, and the data are not presented. All model component data taken at $M_\infty = 0.9$ indicate that a positive value of $(T_\infty - T_{DP})$ is required to ensure no data variance with humidity. A differential temperature of about 10°F is sufficient to obtain accurate aerodynamic data for either model at Mach number 0.9.

At Mach number 1.2, the effect of moisture appears to be coupled with model size (length and relaxation time) since the 1/9-scale model axial force data are essentially insensitive to variations in $(T_\infty - T_{DP})$, and the 1/4-scale model data reach a constant value at $(T_\infty - T_{DP}) \geq 15°F$. The pitching moment and normal force data for both models are invariant with moisture content if $(T_\infty - T_{DP}) \geq -10°F$.

The difference between data obtained at the wettest and driest conditions at Mach numbers 0.9 and 1.2 is presented in Fig. 21 as a function of model angle of attack. At Mach number 0.9 the effect of varying moisture content in the flow would have contributed to data scatter but would not have significantly influenced the zero lift, trim, or drag.

At Mach number 1.2, both the test article trim (ΔC_m shift) and axial force (ΔC_A) indicate a humidity effect which is a function of model size. Price (Ref. 7) has shown that the shock reflection pattern from the model and tunnel walls on the 1/4- and 1/9-scale models is different and could influence the test results at Mach numbers between 1.0 and 1.2. Thus, the shock reflection phenomenon interrelated with moisture condensation could influence the data obtained on models the size of the 1/4-scale test article at Mach number 1.2 in Tunnel 16T.
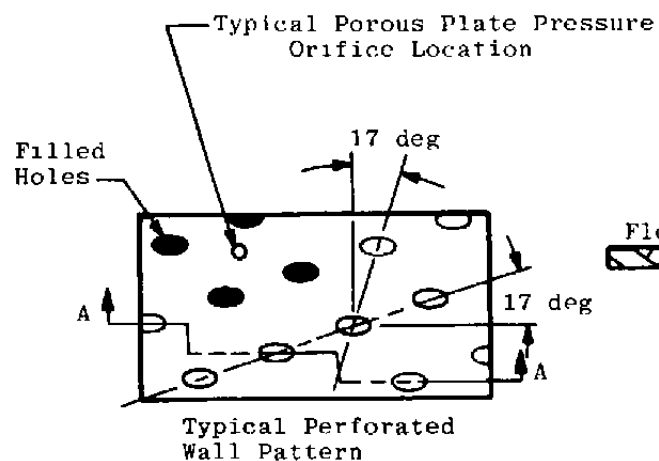
5.0 CONCLUDING REMARKS

A 1/9- and 1/4-scale model of a fighter aircraft was tested in the Propulsion Wind Tunnel (16T) to define the influence of model size, location, and attitude, and humidity and Reynolds number on the tunnel test conditions. Following is a summary of the results from this investigation.

1. The model size, location, and attitude do not influence the free-stream conditions approaching the model in Tunnel 16T for the range of conditions tested.

2. The use of a calibration procedure based on tunnel wall pressure data at Tunnel Station -4 provides no significant improvement over the currently used calibration algorithm.

3. The current Reynolds number correction incorporated in the calibration algorithm appears valid for the instrumentation in use. Refined corrections should be investigated for Mach number 0.6 if more accurate measurements were available.

4. For static stability and performance tests, Tunnel 16T should be operated at free-stream static temperatures above the dewpoint temperature at the supersonic Mach numbers to minimize humidity effects on the model data. Since Tunnel 16T is limited to total temperature less than 160°F, additional drier capacity could be used to reach that condition at Mach numbers greater than 1.2.

In addition further studies would be desirable to define the humidity effects at higher Mach number (1.3 to 1.6) in Tunnel 16T, verify if these effects are configuration unique, and determine if the data can be corrected to dry condtions if the variation of model aerodynamics with humidity is established. A theoretical prediction rationale and program could also be developed to provide estimates of humidity effects on test articles in Tunnel 16T and extended to provide corrective increments for conditions where humidity effects are still present.

REFERENCES

1. *Test Facilities Handbook* (Eleventh Edition). "Propulsion Wind Tunnel Facility, Vol. 4." Arnold Engineering Development Center, June 1979.

2. Jackson, F. M., III." Calibration of the AEDC-PWT 16-ft Transonic Tunnel Aerodynamic Test Section at Various Reynolds Numbers." AEDC-TR-78-60 (AD-A065112), February 1979.

3. Abernethy, R. B. and Thompson, J. W., Jr. "Handbook - Uncertainty in Gas Turbine Measurements." AEDC-TR-73-5 (AD755356), February 1973.

4. Gunn, J. A. "Check Calibration of the AEDC 16-ft Transonic Tunnel." AEDC-TR-66-80 (AD633277), May 1966.

5. Spratley, A. V. "Reynolds Number and Nozzle Afterbody Configuration Effects on Model Forebody and Afterbody Drag." AIAA Paper No. 77-103, 1977.

6. Nichols, James H. "Determination of Optimum Operating Parameters for the PWT 16-ft Transonic Circuit Utilizing One-Percent Bodies of Revolution." AEDC-TN-59-100 (AD 225362), September 1959.

7. Price, Earl A., Jr. "An Investigation of F-16 Nozzle-Afterbody Forces at Transonic Mach Numbers with Emphasis on Model Scale Effects." AEDC-TR-80-57, to be published.

Typical Porous Plate Pressure
Orifice Location

Filled
Holes

17 deg

17 deg

A

A

Typical Perforated
Wall Pattern

Flow

60 deg

Section A-A

① 20 Orifices (Sta 1 to 20) 1 ft West of
Bottom Wall Centerline (PBW1 to PBW20)

② 20 Orifices (Sta 1 to 20) 1 ft West of
Top Wall Centerline (PTW1 to PTW20)
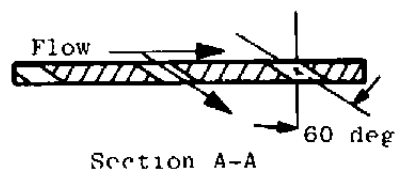
6-percent Open Area
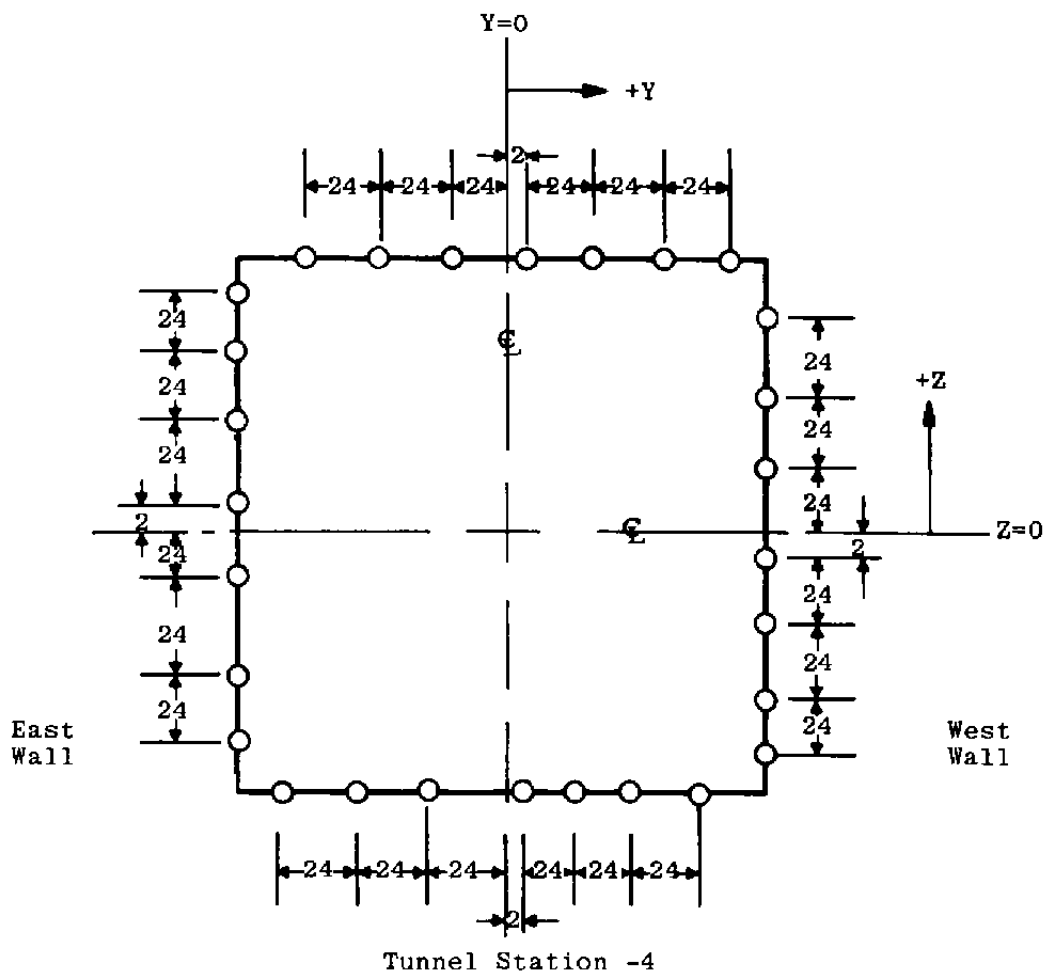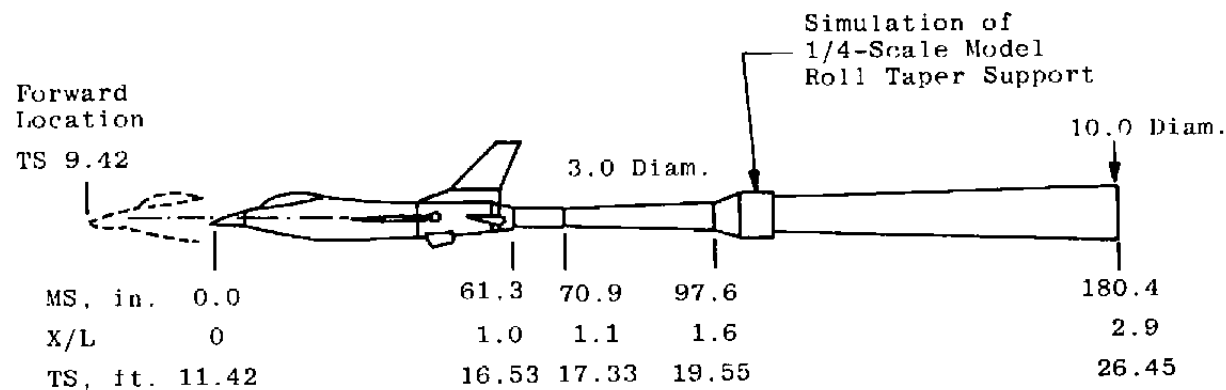Hole Diameter = 0.75 in.
Plate Thickness = 0.75 in.

Solid
Area

Perforated
Walls

Solid Diverged Wall Section
to Alleviate Strut Blockage

Model Support
Strut

Ç

Sta
-10

Sta
-4

Sta
0

Sta
7.83

Sta
28

Sta
40
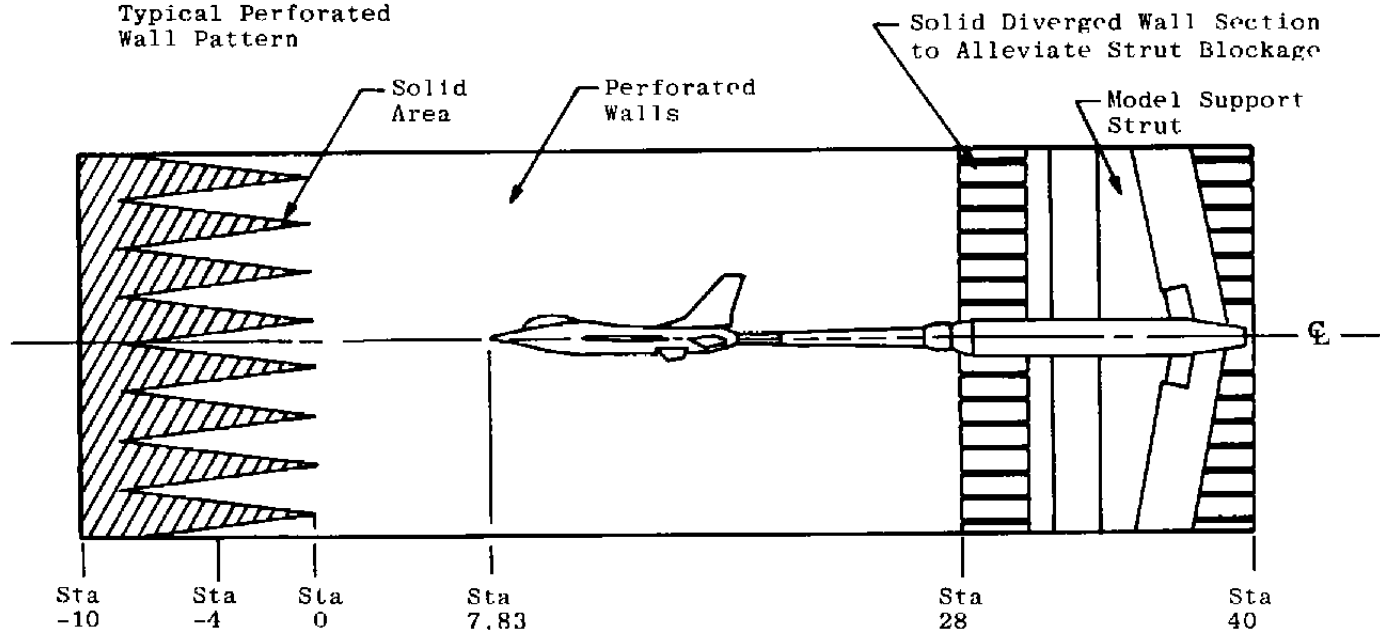
Figure 1. 1/4-scale model on the 16T sting support system.

Figure 2. Wind tunnel nozzle wall static pressure orifice locations at at tunnel station -4.

Simulation of
1/4-Scale Model
Roll Taper Support

Forward
Location

TS 9.42

10.0 Diam.

3.0 Diam.

MS, in.	0.0	61.3	70.9	97.6	180.4
X/L	0	1.0	1.1	1.6	2.9
TS, ft.	11.42	16.53	17.33	19.55	26.45

a. 1/9-Scale Model.

10.0 Diam.

6.5 Diam.

MS, in.	0.0	138.1	156.9	223.4
X/L	0	1.0	1.1	1.6
TS, ft.	7.83	19.34	20.91	26.45
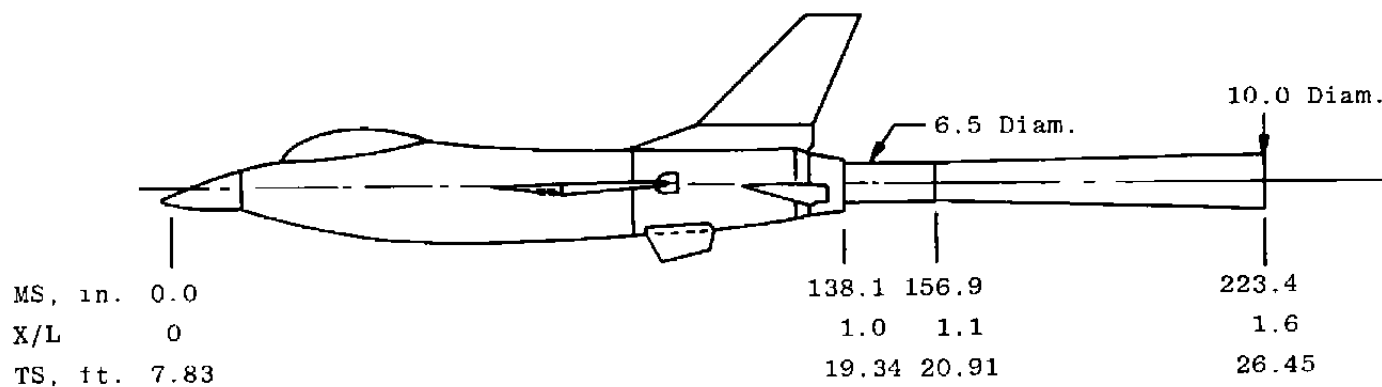
b. 1/4-Scale Model.

Figure 3. Model and support system location in tunnel 16T.
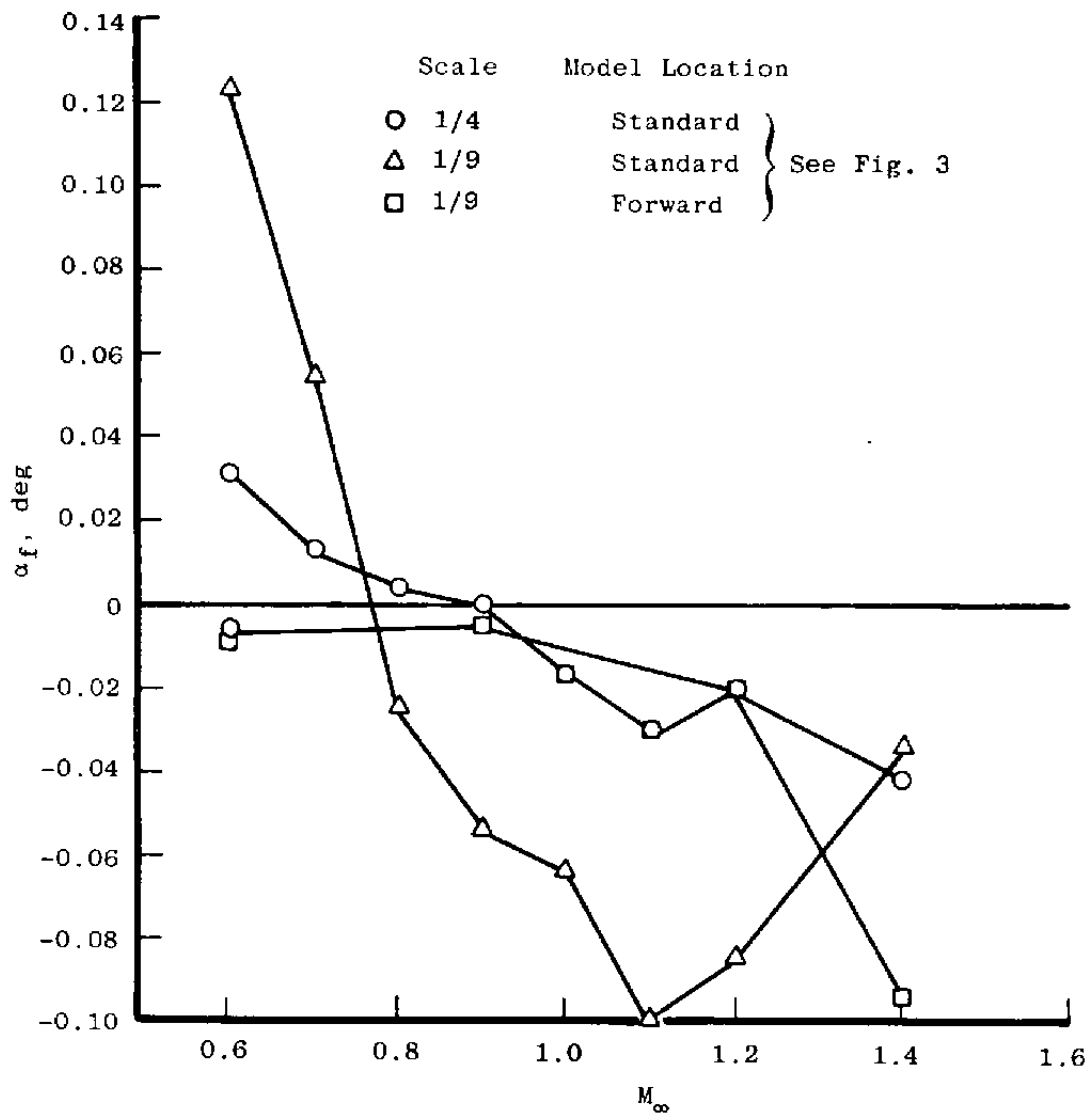
Figure 4. Flow angularity in tunnel 16T for the two sting support models.
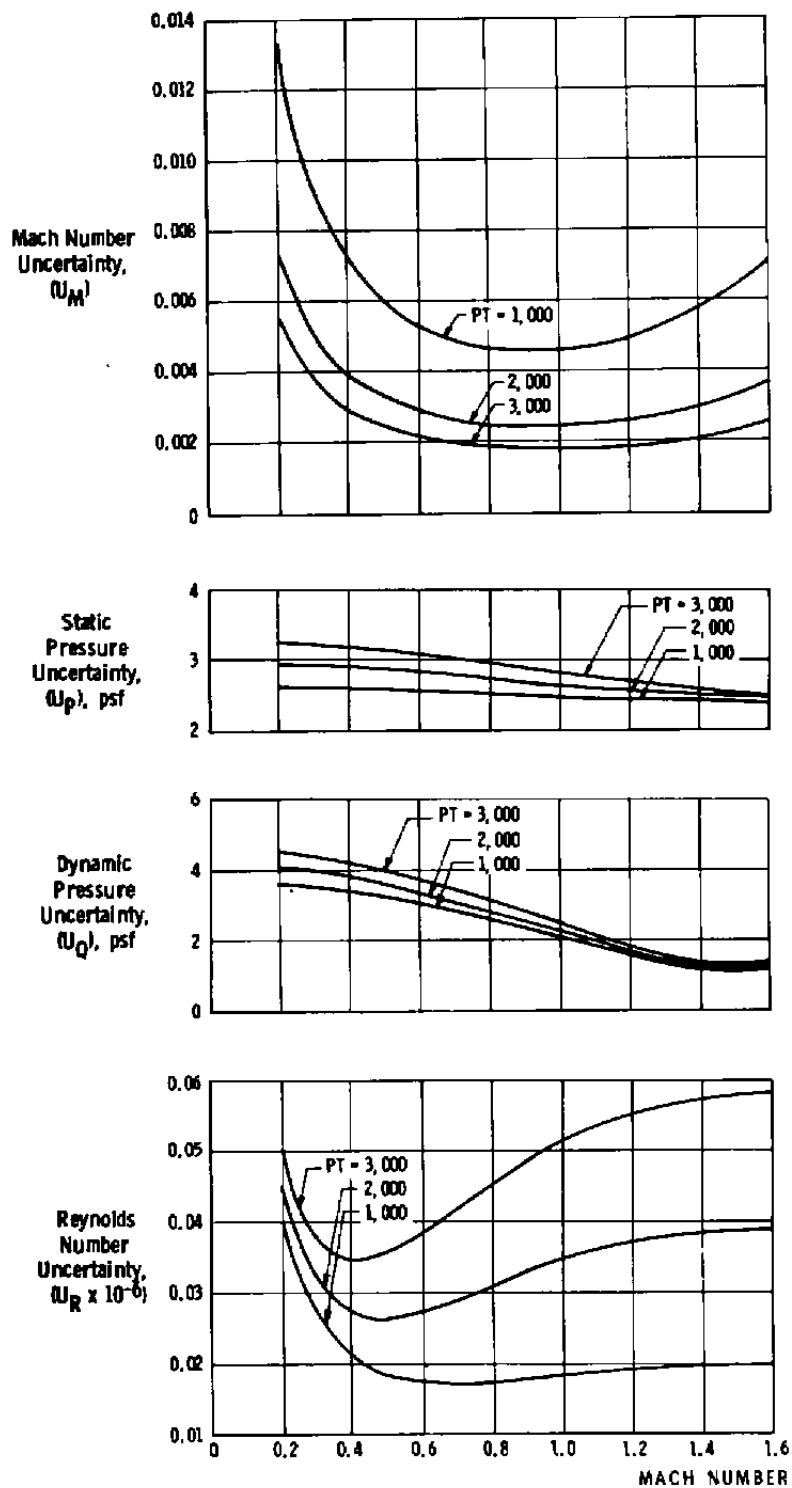
Figure 5. Estimated uncertainties in wind tunnel parameters.

$$\Delta C_p = \left(C_{p_{avg}}\right)_{1/4 \text{ scale}} - \left(C_{p_{avg}}\right)_{1/9 \text{ scale}}$$
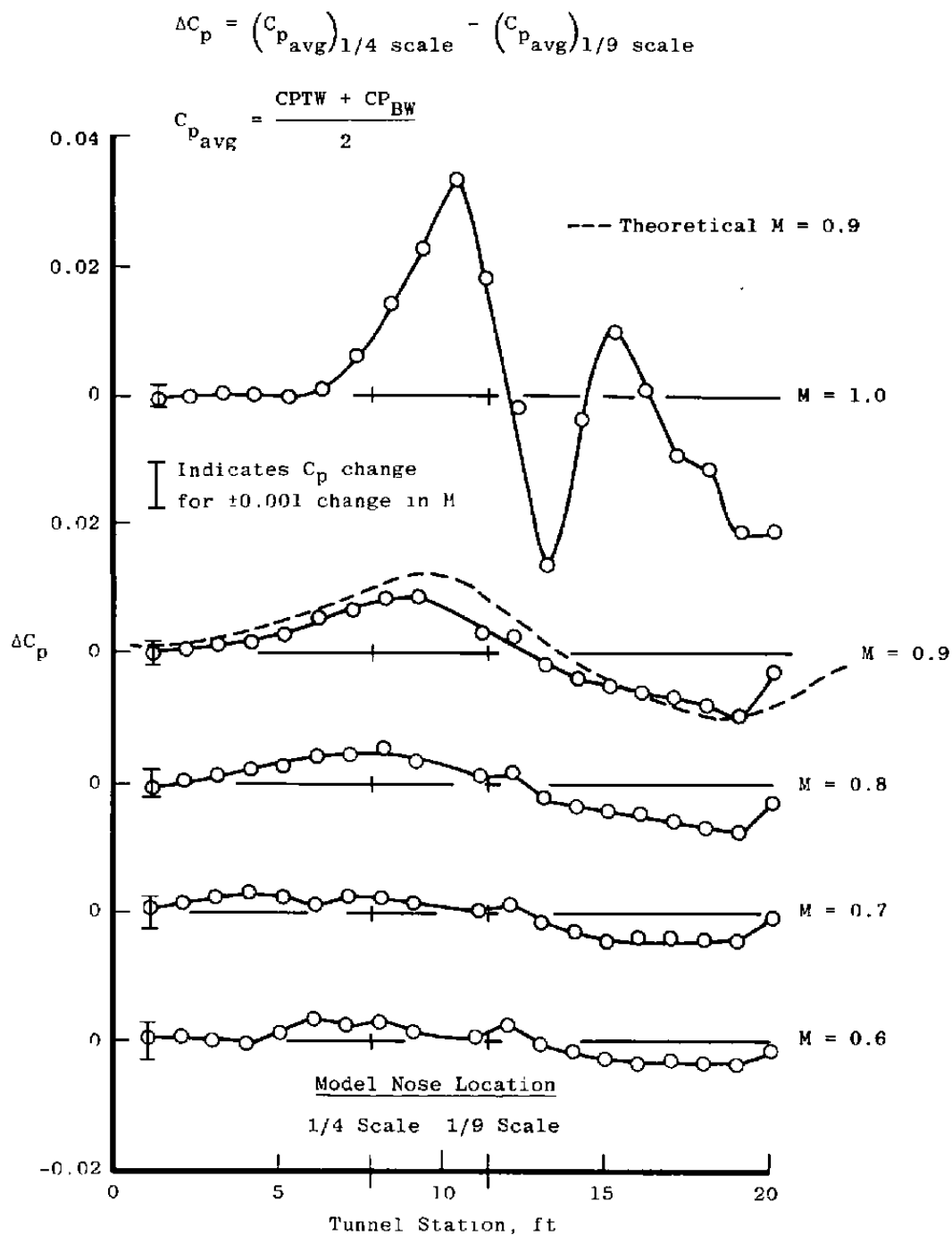
$$C_{p_{avg}} = \frac{CPTW + CP_{BW}}{2}$$

a. M ≤ 1.0

Figure 6. Effect of model size on the test section wall static pressures.

$$\Delta C_p = \left(C_{p_{avg}}\right)_{1/4 \text{ scale}} - \left(C_{p_{avg}}\right)_{1/9 \text{ scale}}$$

$$C_{p_{avg}} = \frac{CPTW + CP_{BW}}{2}$$
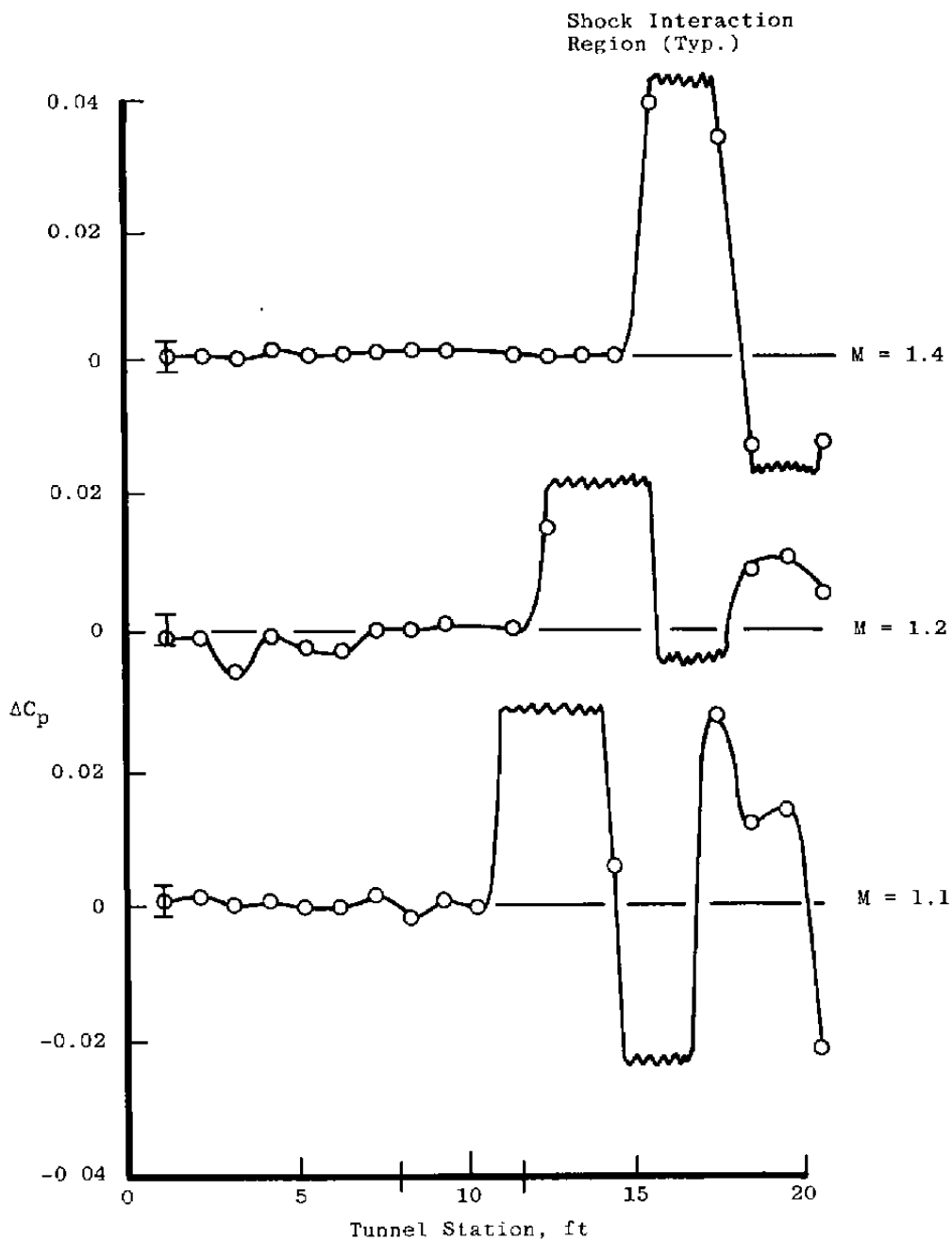
b. M > 1.0
Figure 6. Concluded.
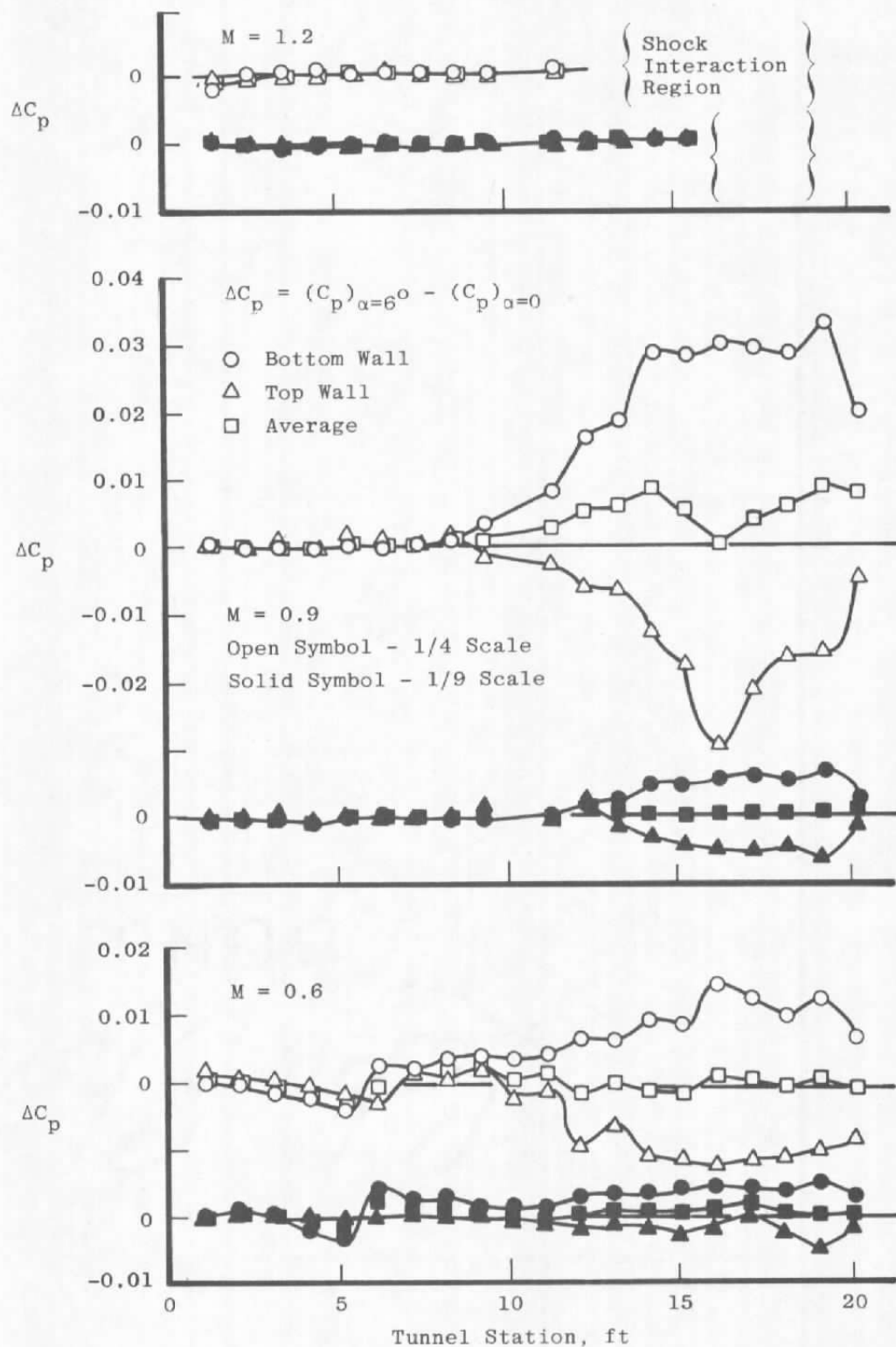
Figure 7. Effect of model attitude on the test section wall
static pressures.

$$\Delta C_p = \left(\frac{CPTW_i + CP_{BW_i}}{2}\right)_{Std} - \left(\frac{CPTW_i + CP_{BW_i}}{2}\right)_{Fwd}$$
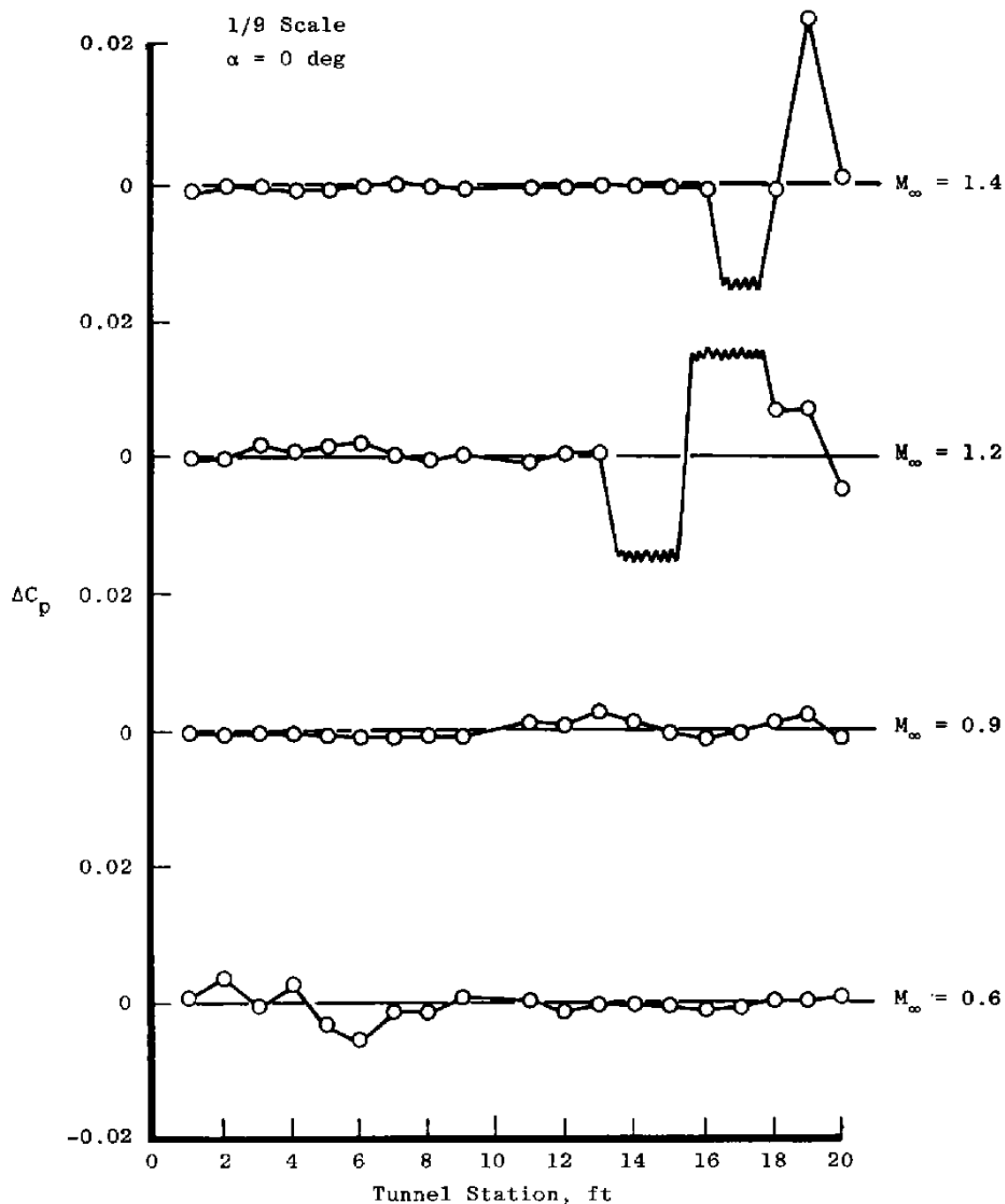
Figure 8. Effect of model location on test section wall static pressures.
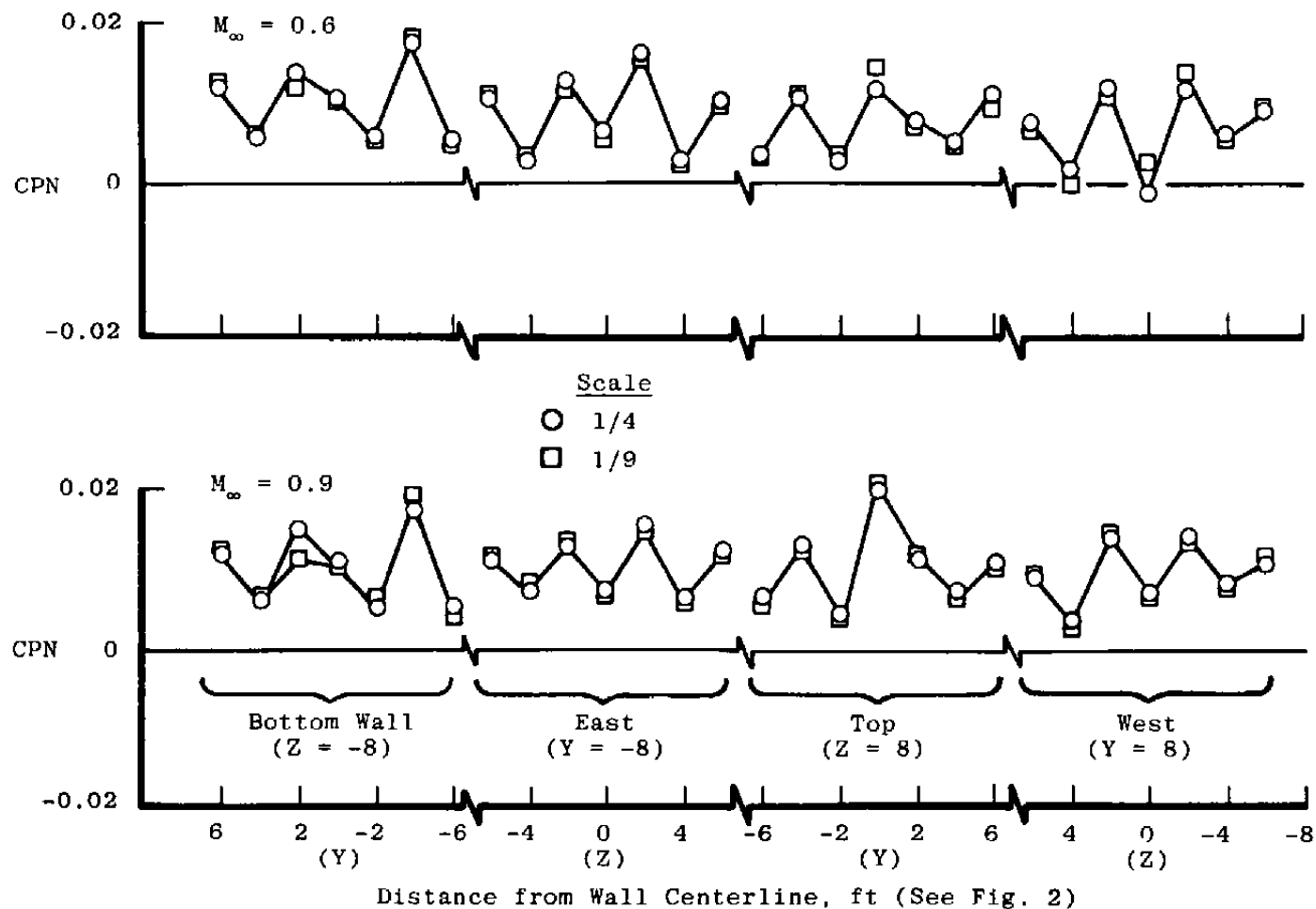
a. Subsonic Mach numbers.

Figure 9. Effect of model size on tunnel station -4 wall
pressure distribution.
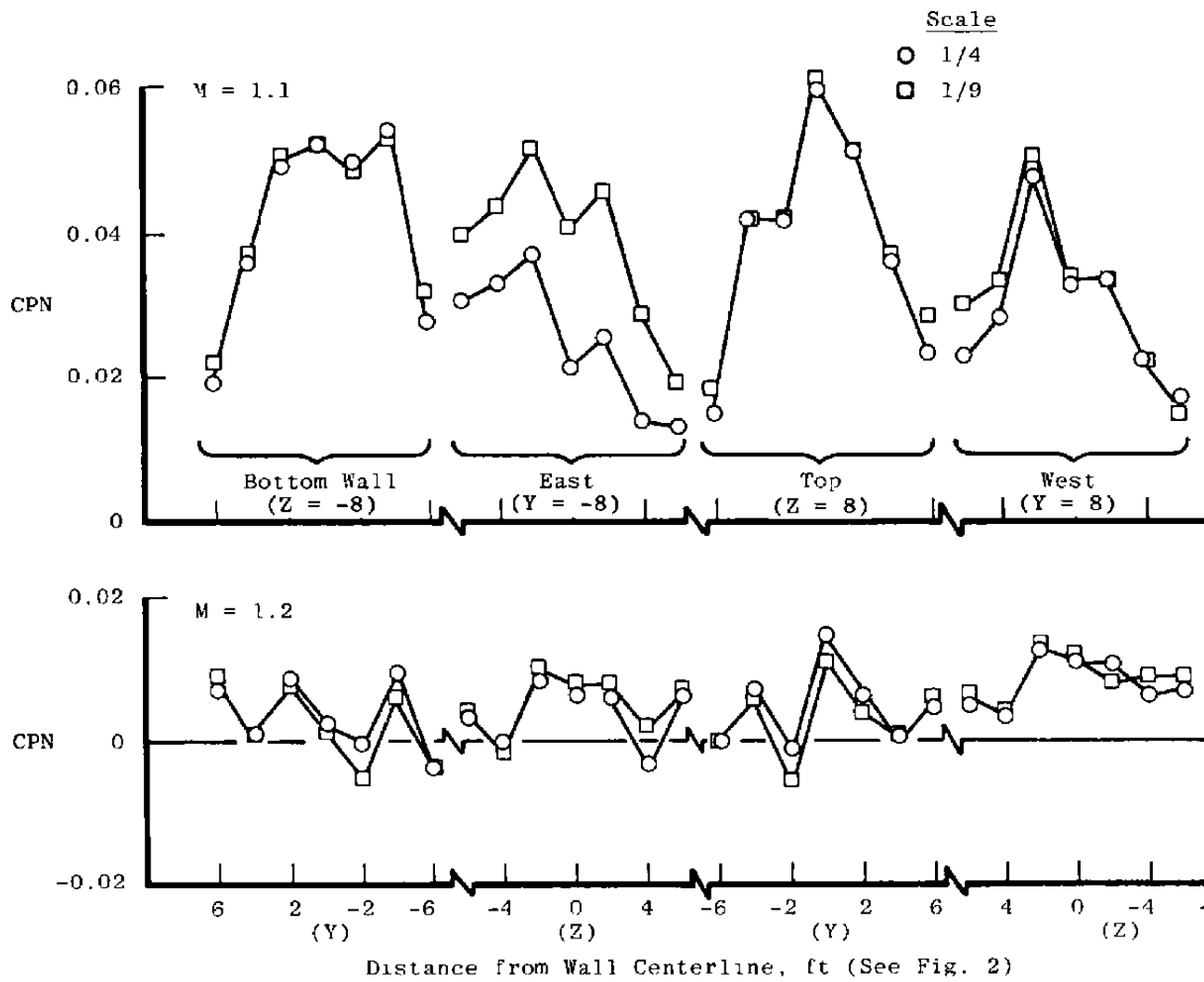
b. Supersonic Mach numbers.
Figure 9. Concluded.
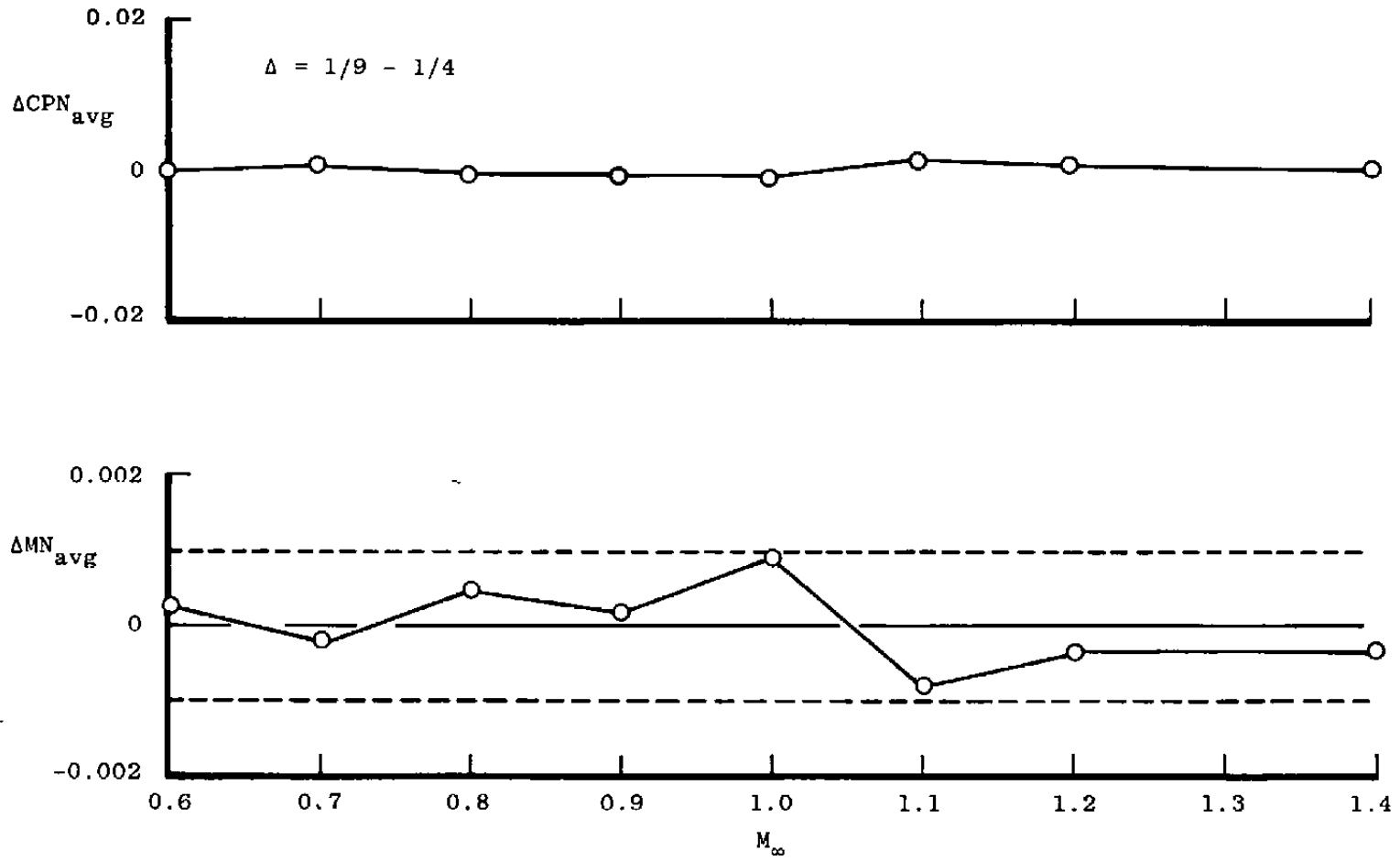
Figure 10. Effect of model size on the average tunnel station -4 parameters.
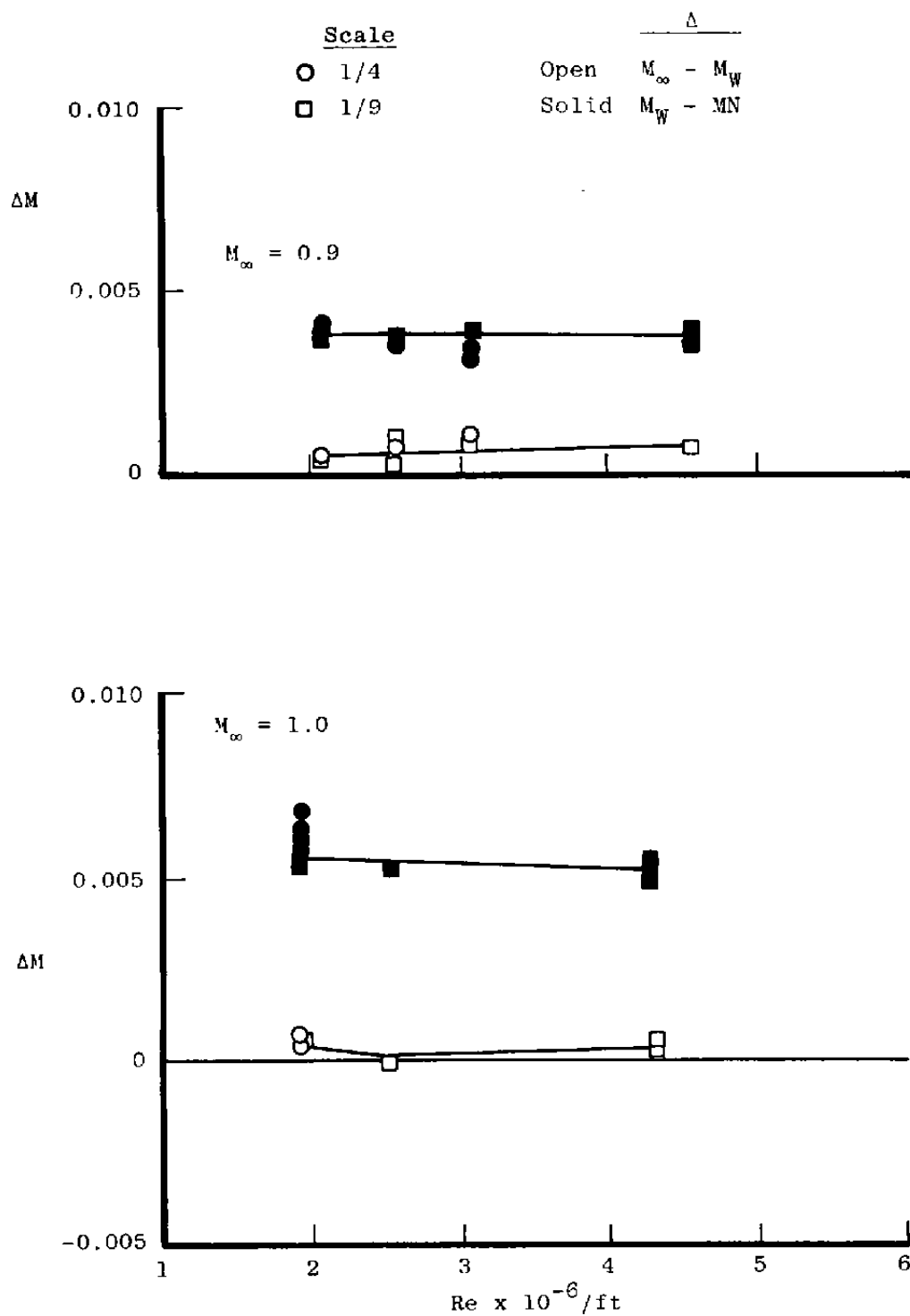
$$\Delta C_p = \left(C_{p_{avg}}\right)_{1/9 \text{ High Re}} - \left(C_{p_{avg}}\right)_{1/9 \text{ Low Re}}$$
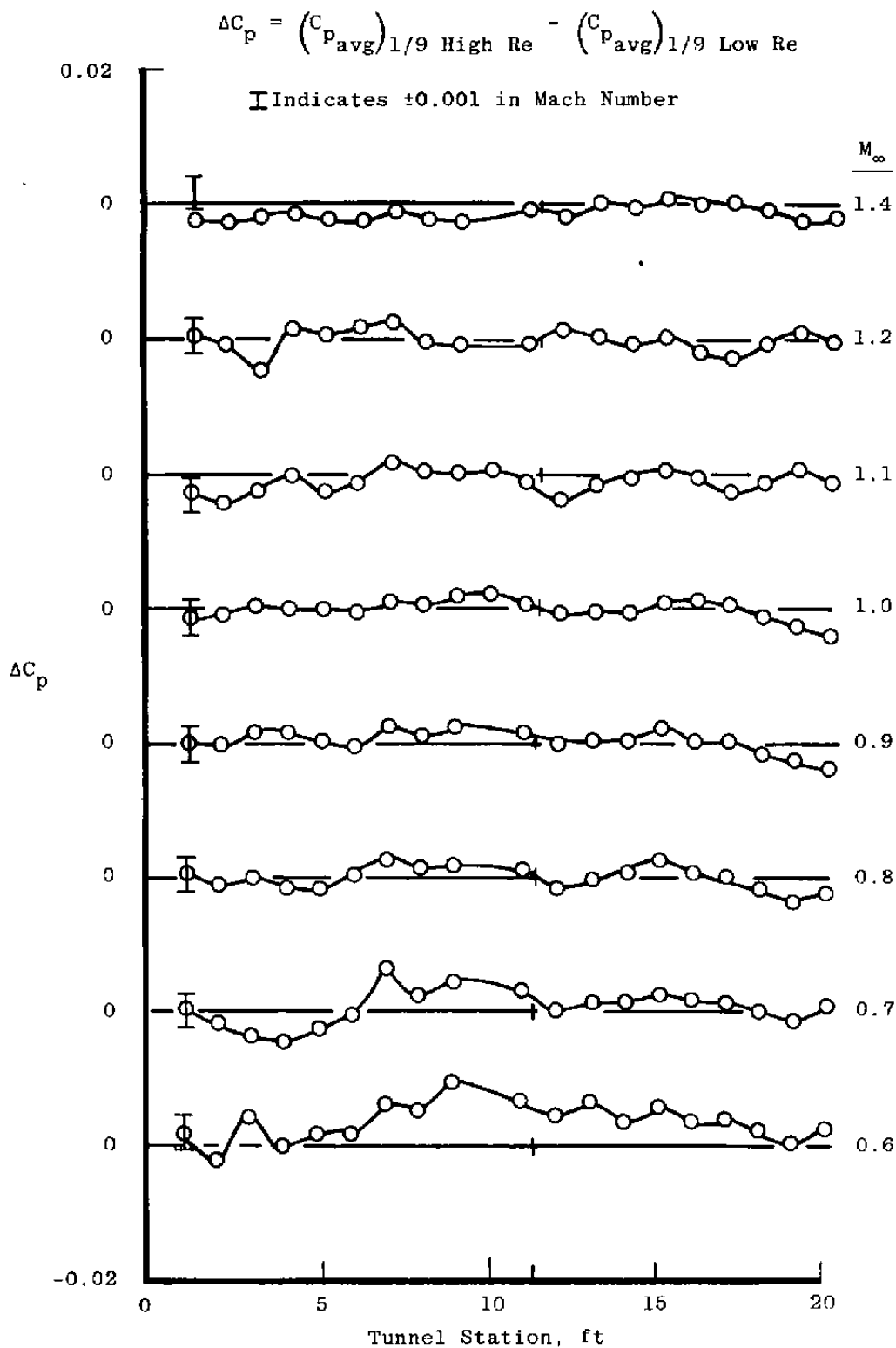
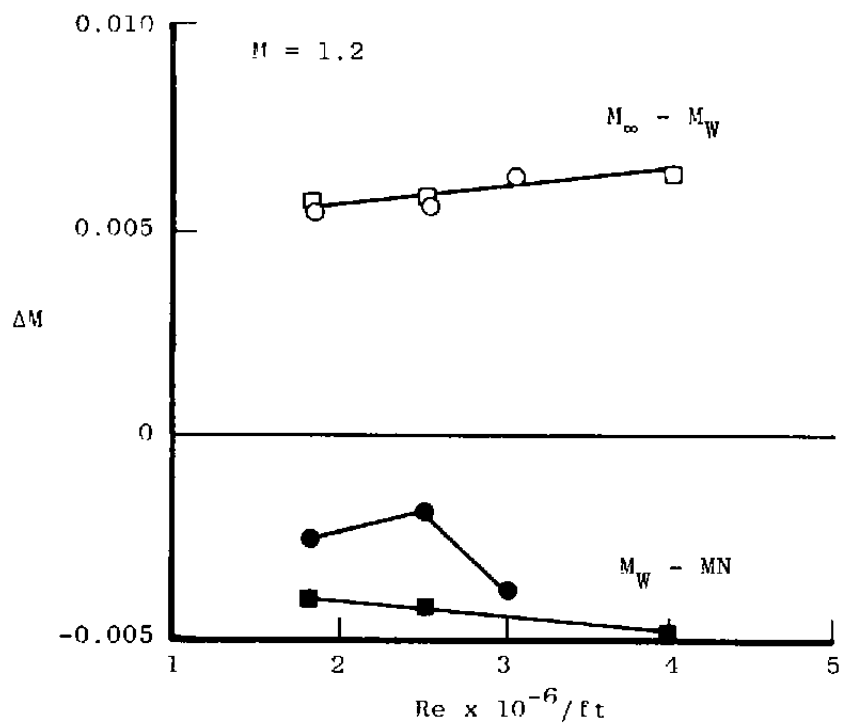Figure 11. Effect of Reynolds number on test section wall static pressures, 1/9-scale model.
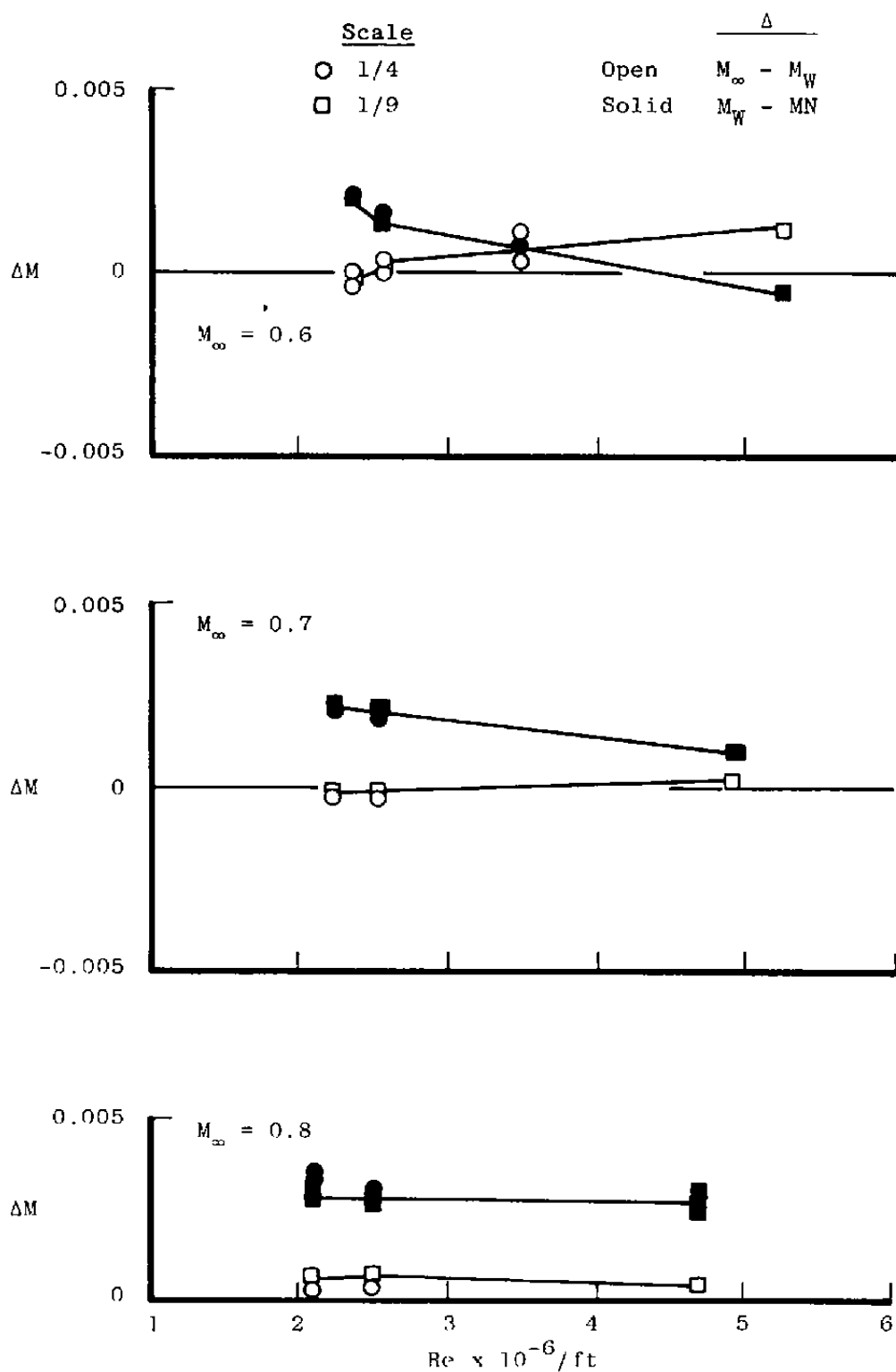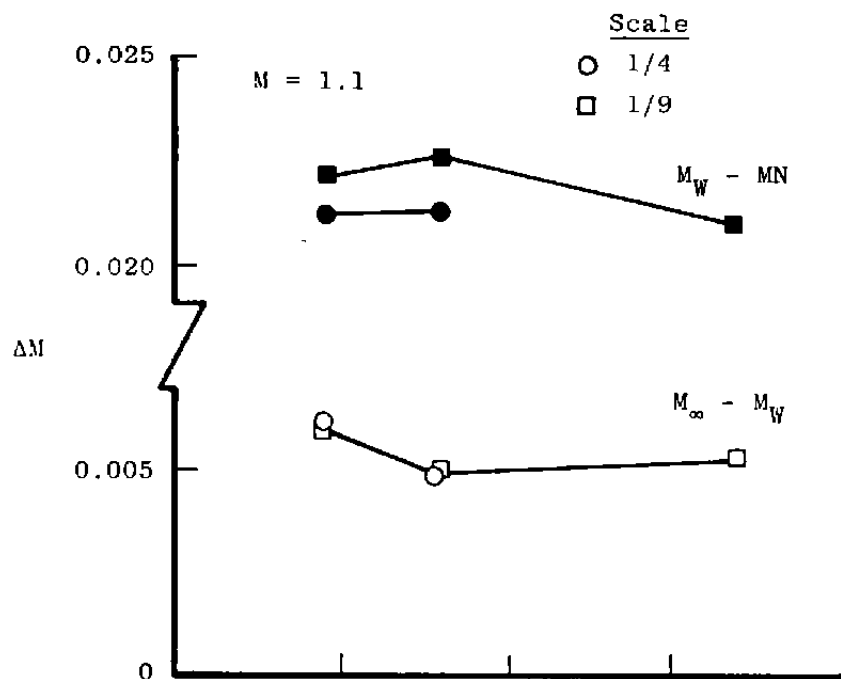
a. M = 0.6, 0.7, 0.8.
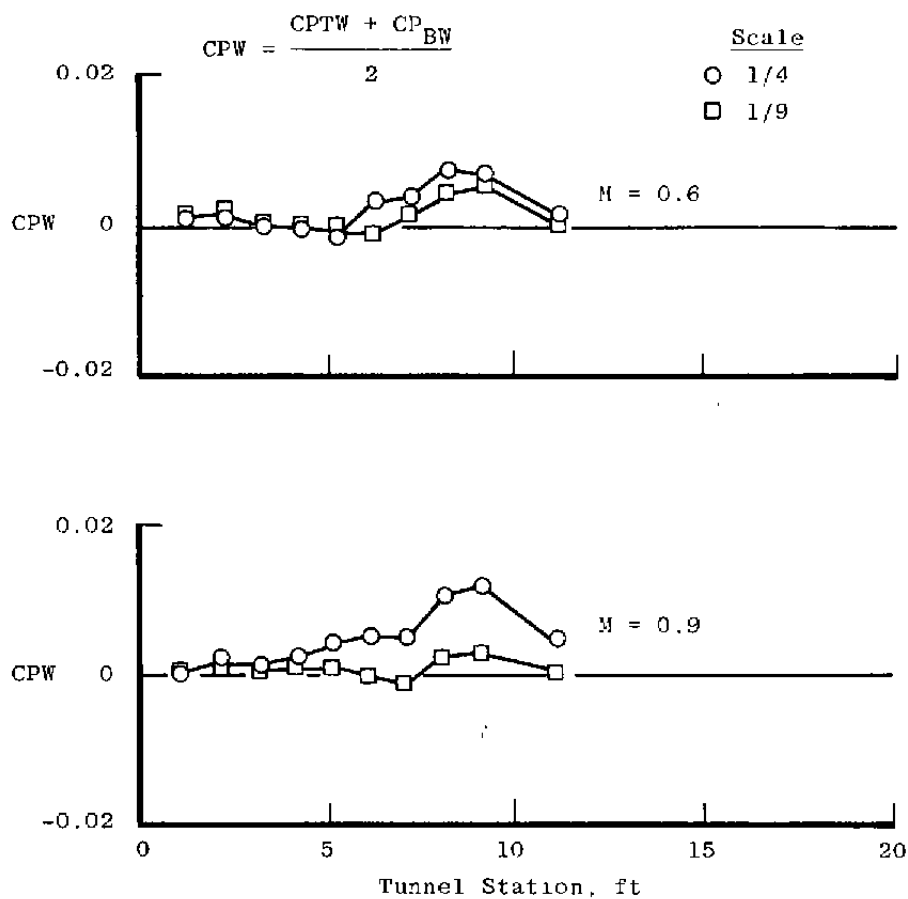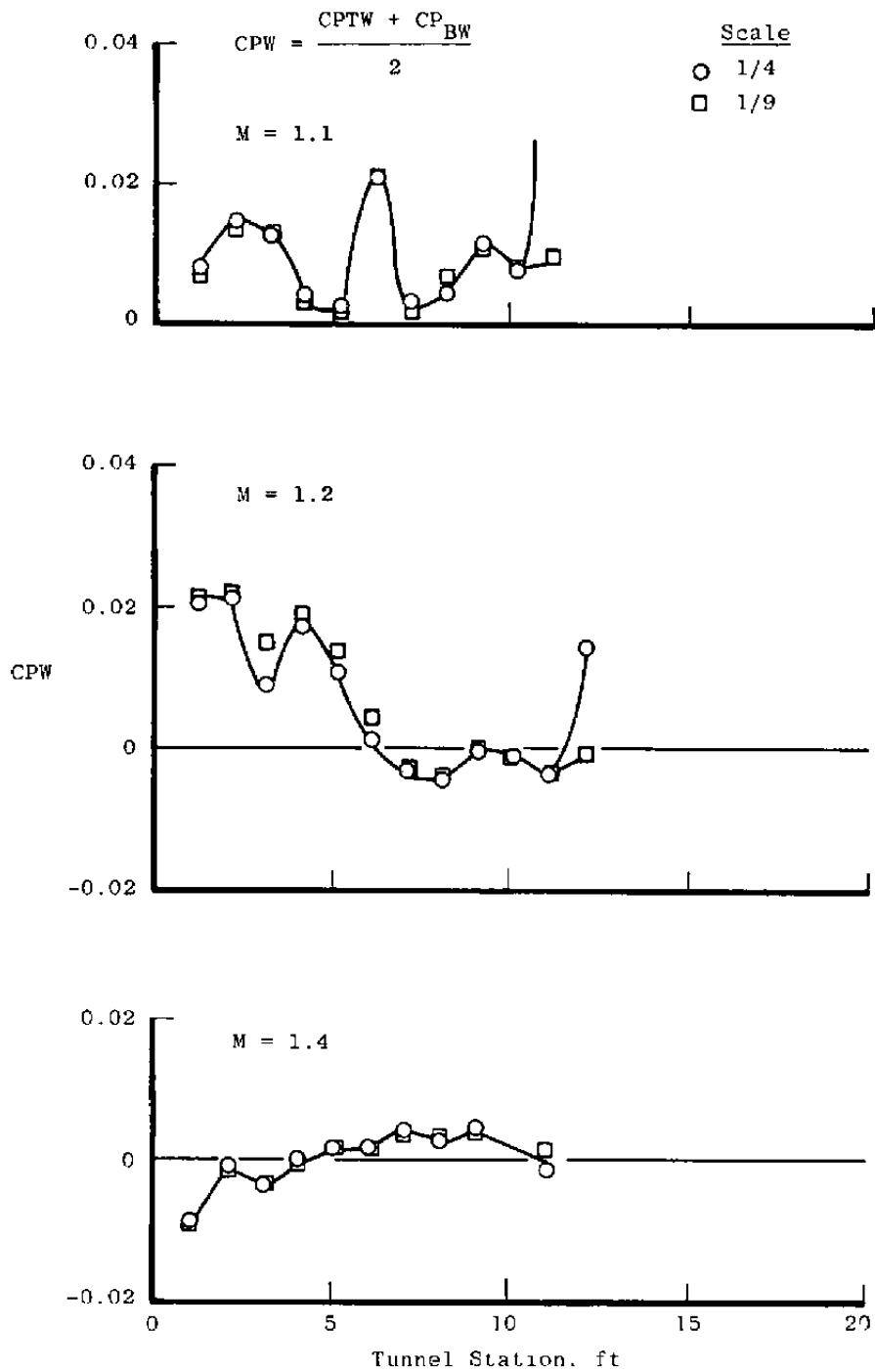Figure 12. Effect of Reynolds number on Mach number parameters.

b. M = 0.9, 1.0.
Figure 12. Continued.

c. M = 1.1, 1.2.
Figure 12. Concluded.

30

a. Subsonic Mach numbers.
Figure 13. Test section wall pressure distribution.

31

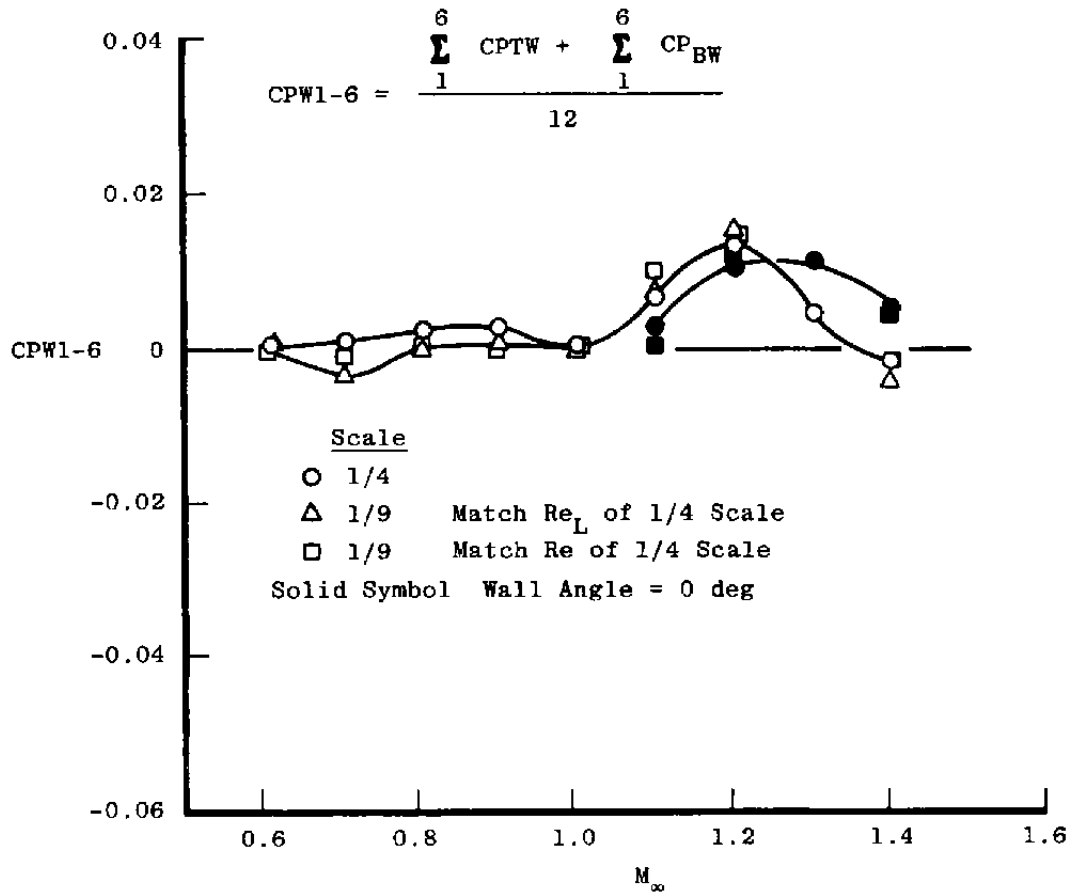b. Supersonic Mach numbers.
Figure 13. Concluded.

Figure 14. Effect of test section wall angle on test section wall static pressures between tunnel stations 1 and 6 ft.

$$\Delta CPN = (CPN)_{\theta=opt} - (CPN)_{\theta=0} \ deg$$

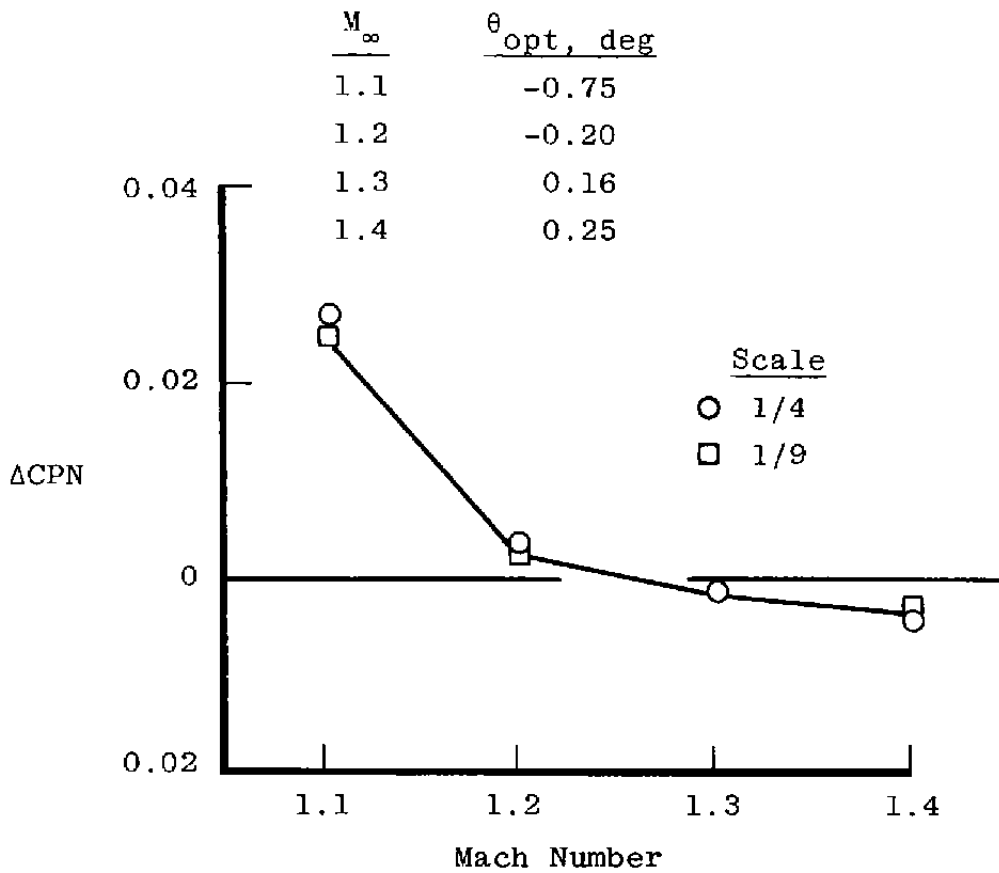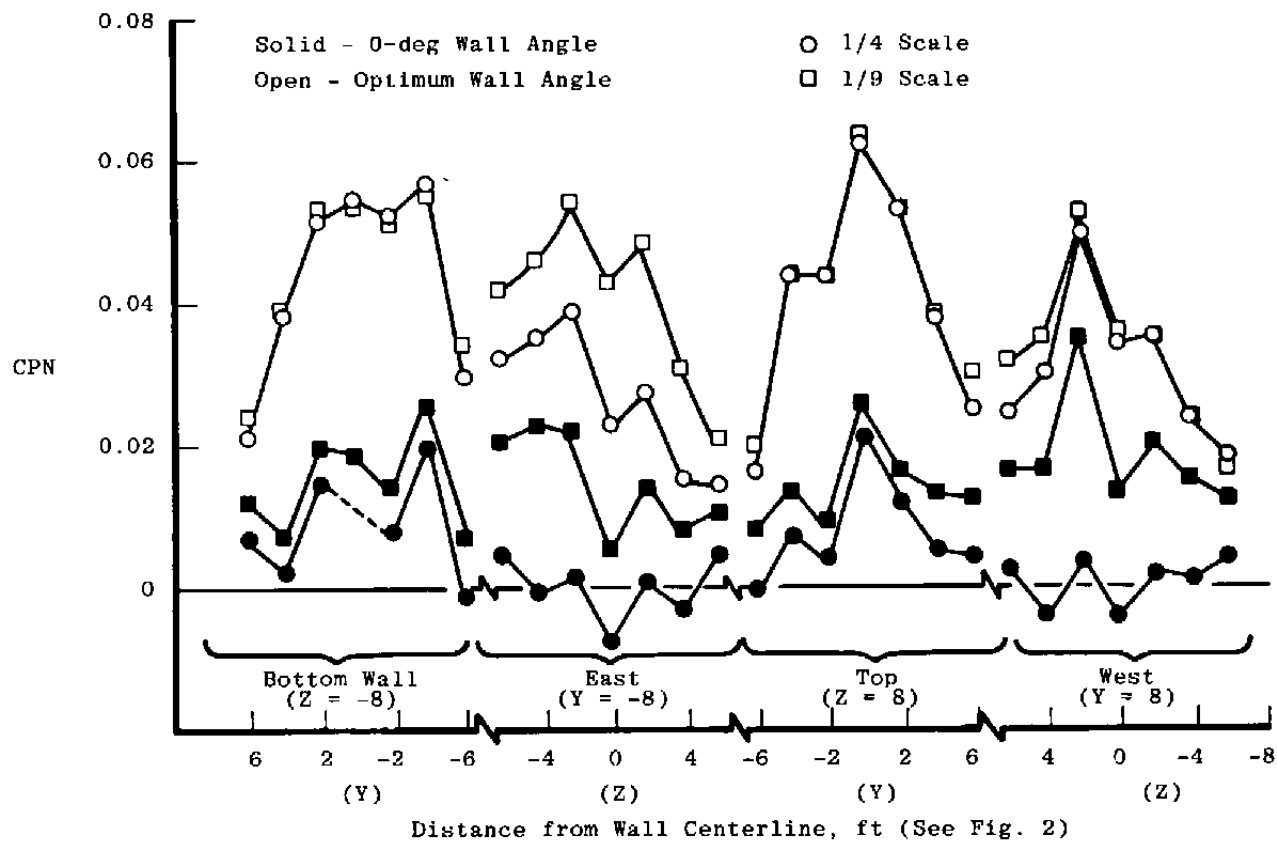| M_∞	$\theta_{opt}, \ deg$
1.1	-0.75
1.2	-0.20
1.3	0.16
1.4	0.25

Figure 15. Effect of wall angle on the tunnel station -4 average pressure.

a. M = 1.1

Figure 16. Effect of wall angle on the tunnel station -4 static
pressure distribution.
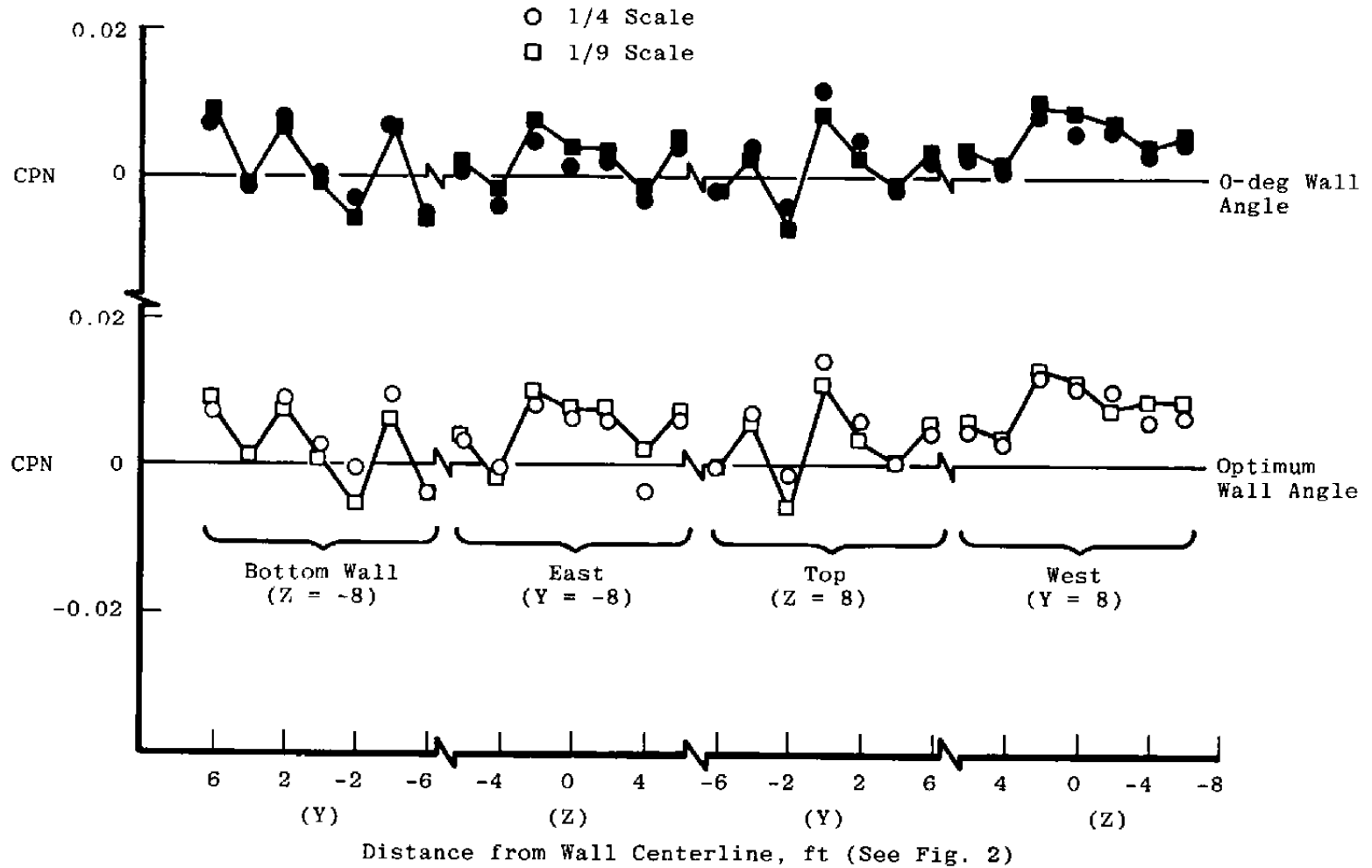
b. M = 1.2.
Figure 16. Concluded.
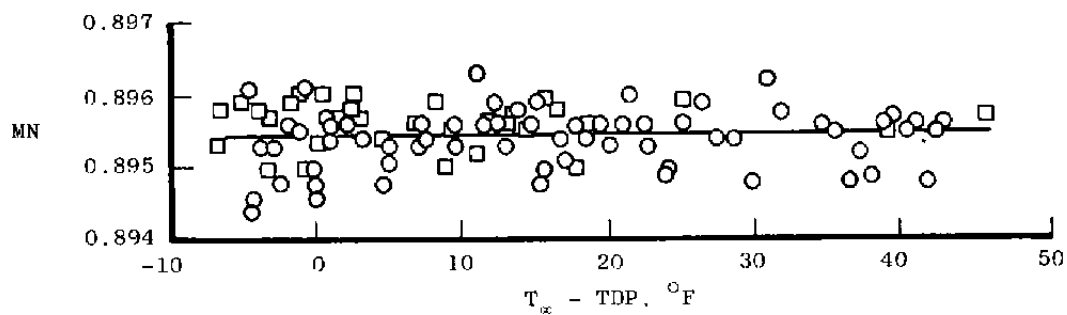
a. M = 0.9.
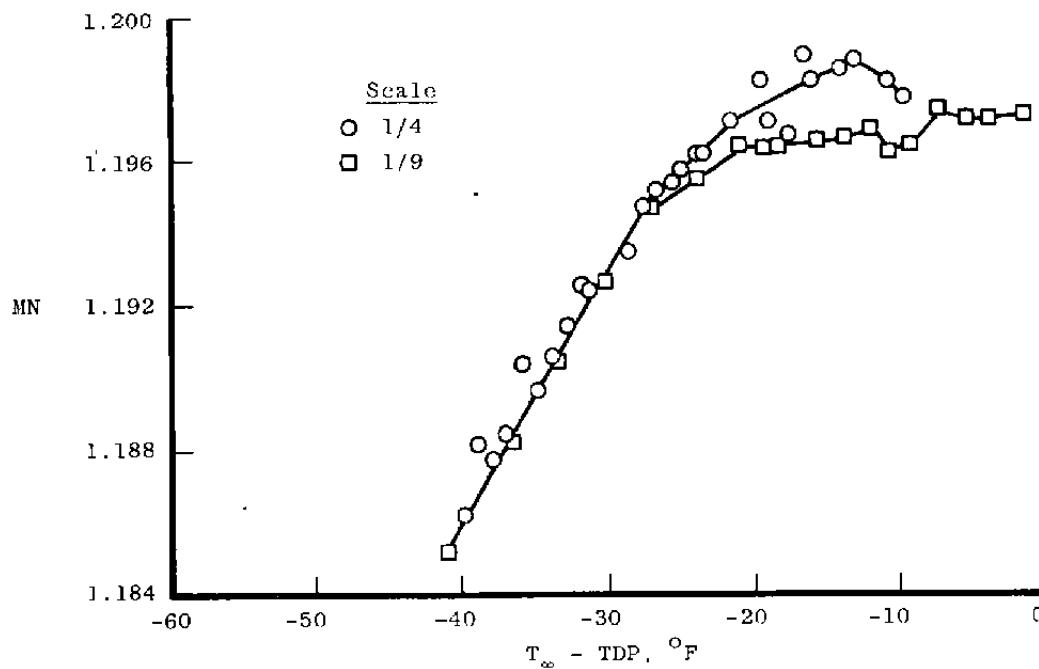
b. M = 1.2

Figure 17. Effect of moisture content on tunnel station -4
average Mach number.
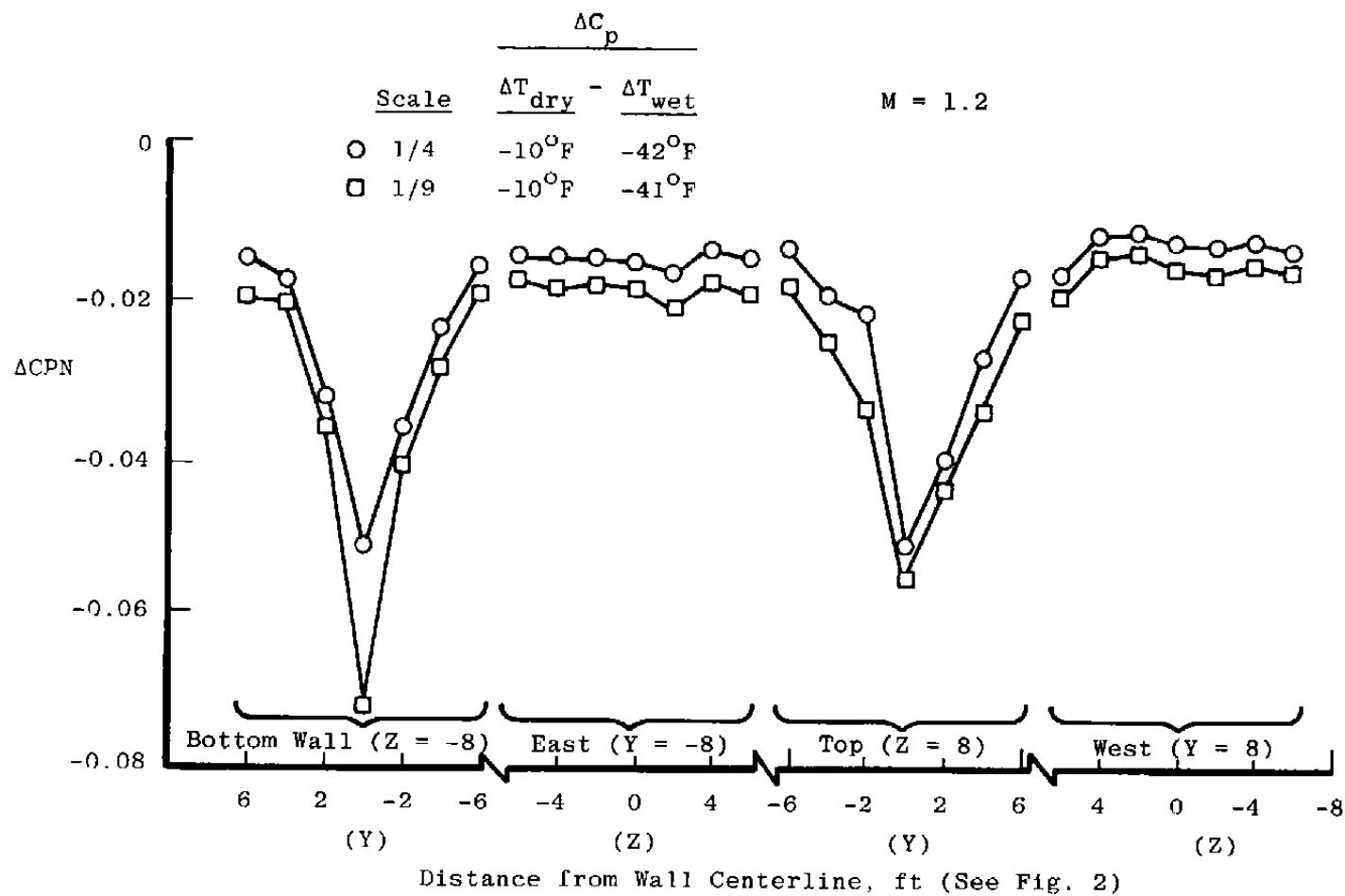
Figure 18. Effect of moisture content on tunnel station -4 wall
pressure distribution.

Figure 19. Effect of moisture content on average wall pressure
between tunnel station 1 and 6 ft.

a. M = 0.9, a = 6 deg.
Figure 20. Effect of moisture content on model aerodynamic coefficients.

b. M = 1.2, a = 6 deg.
Figure 20. Concluded.

a. M = 0.9.

Figure 21. Effect of moisture content on model aerodynamic coefficients as a function of angle of attack.

b. M = 1.2
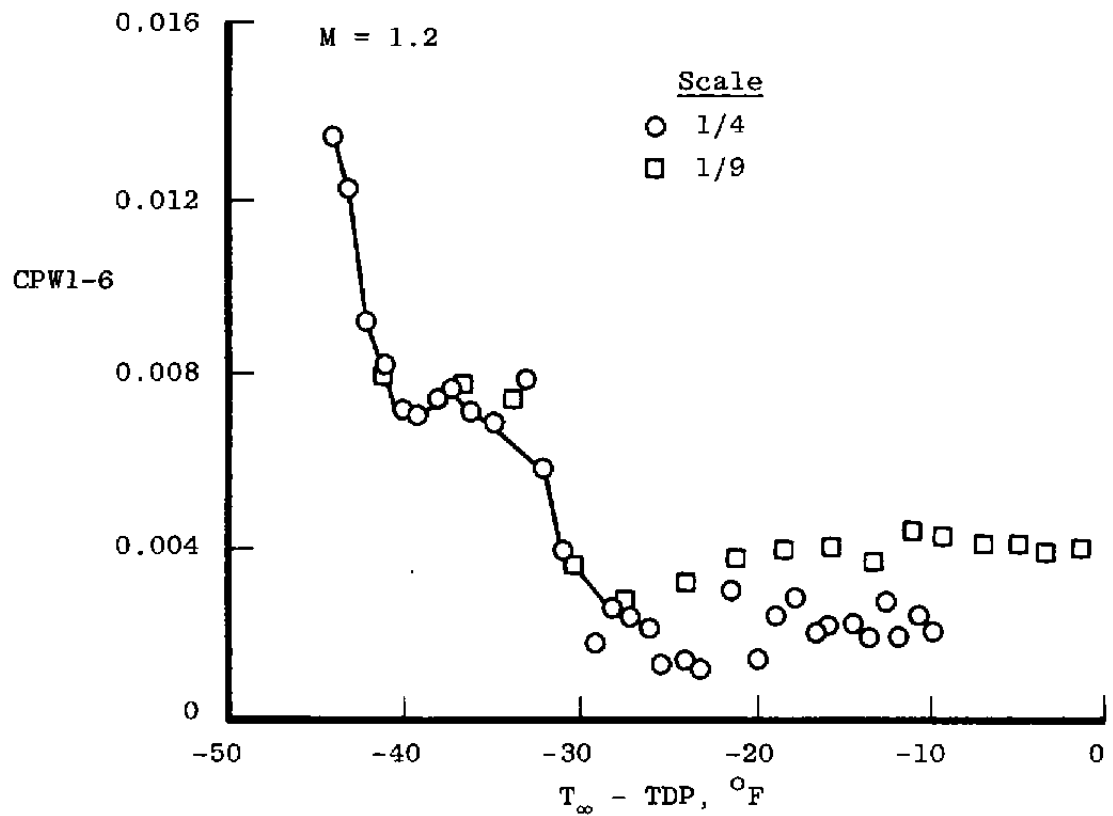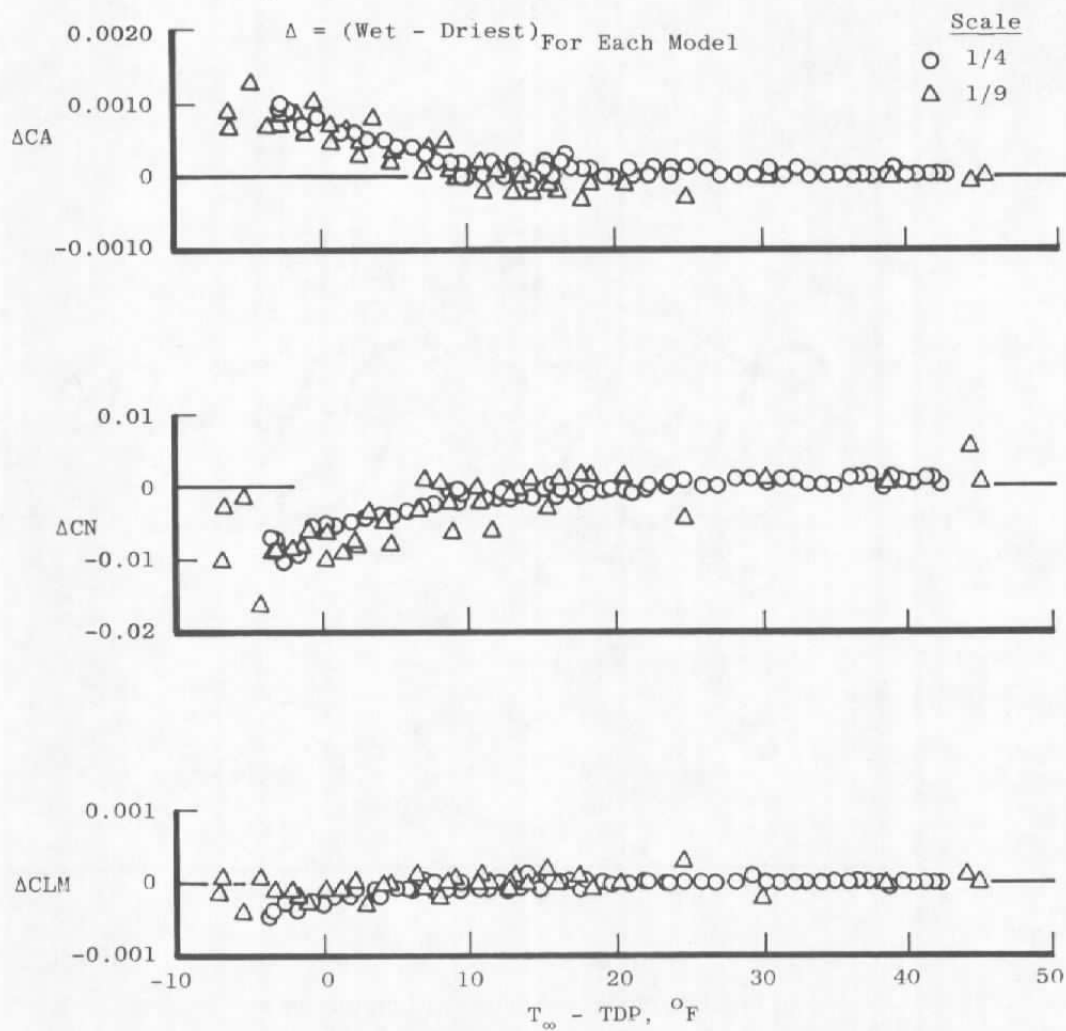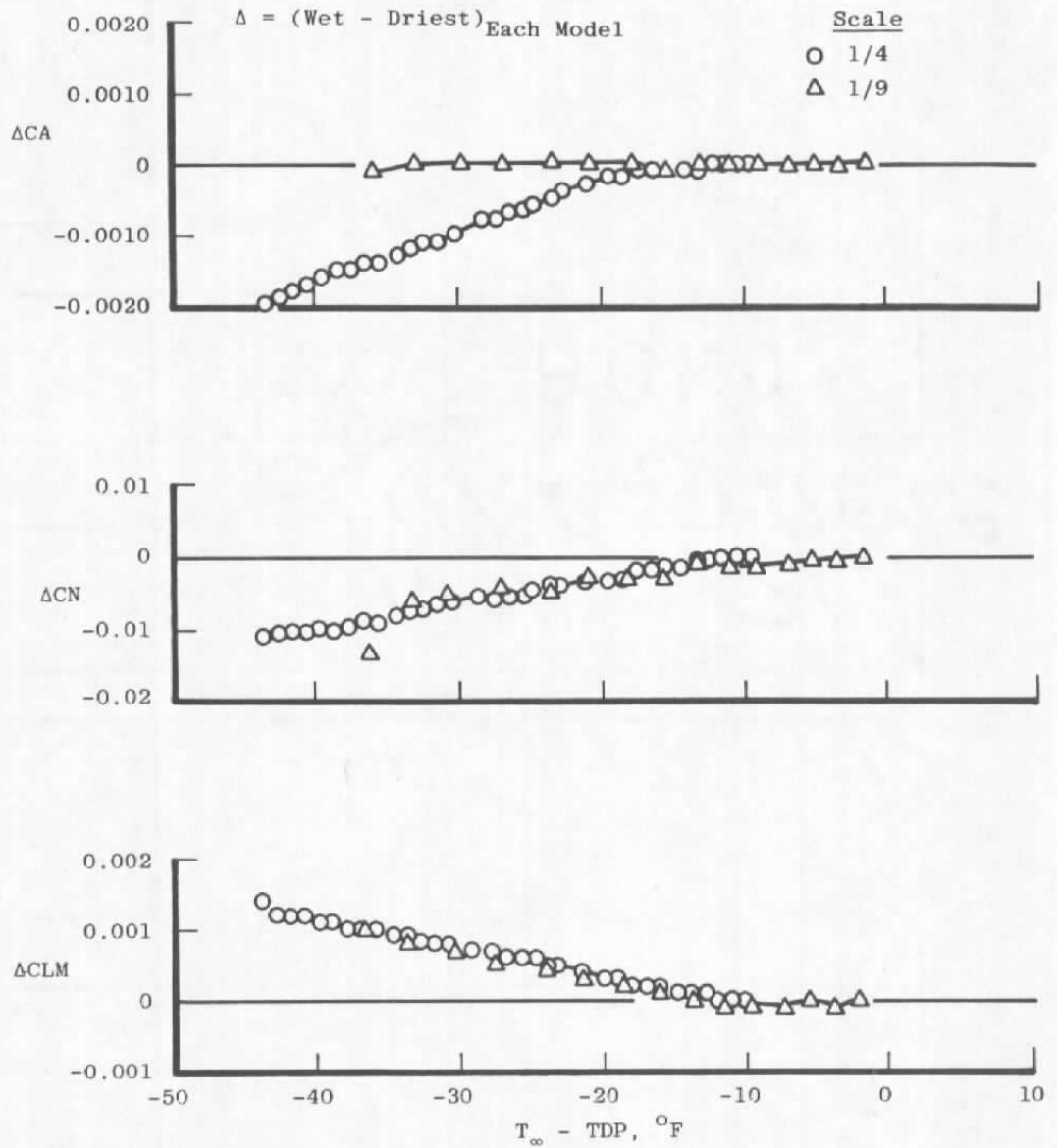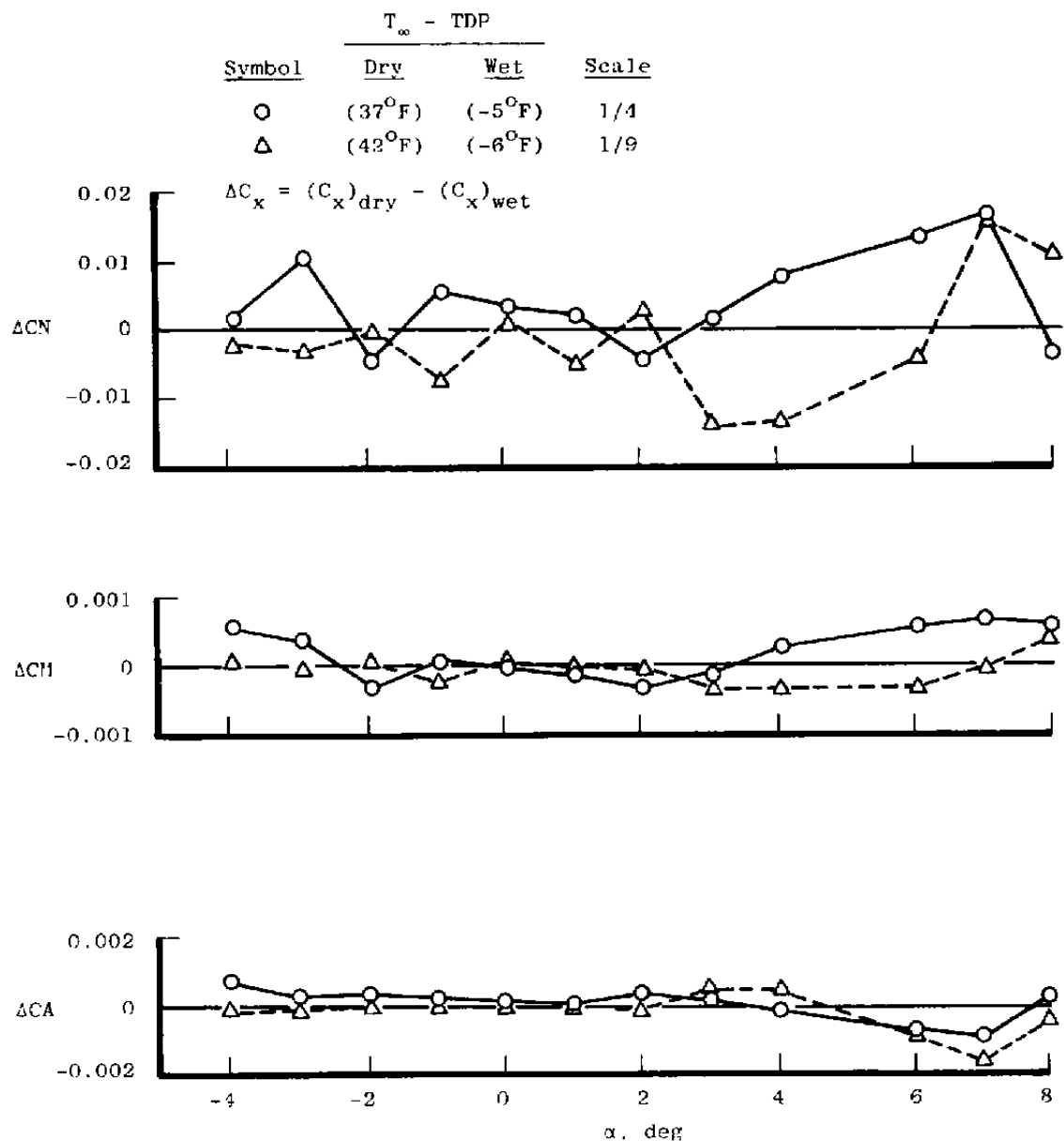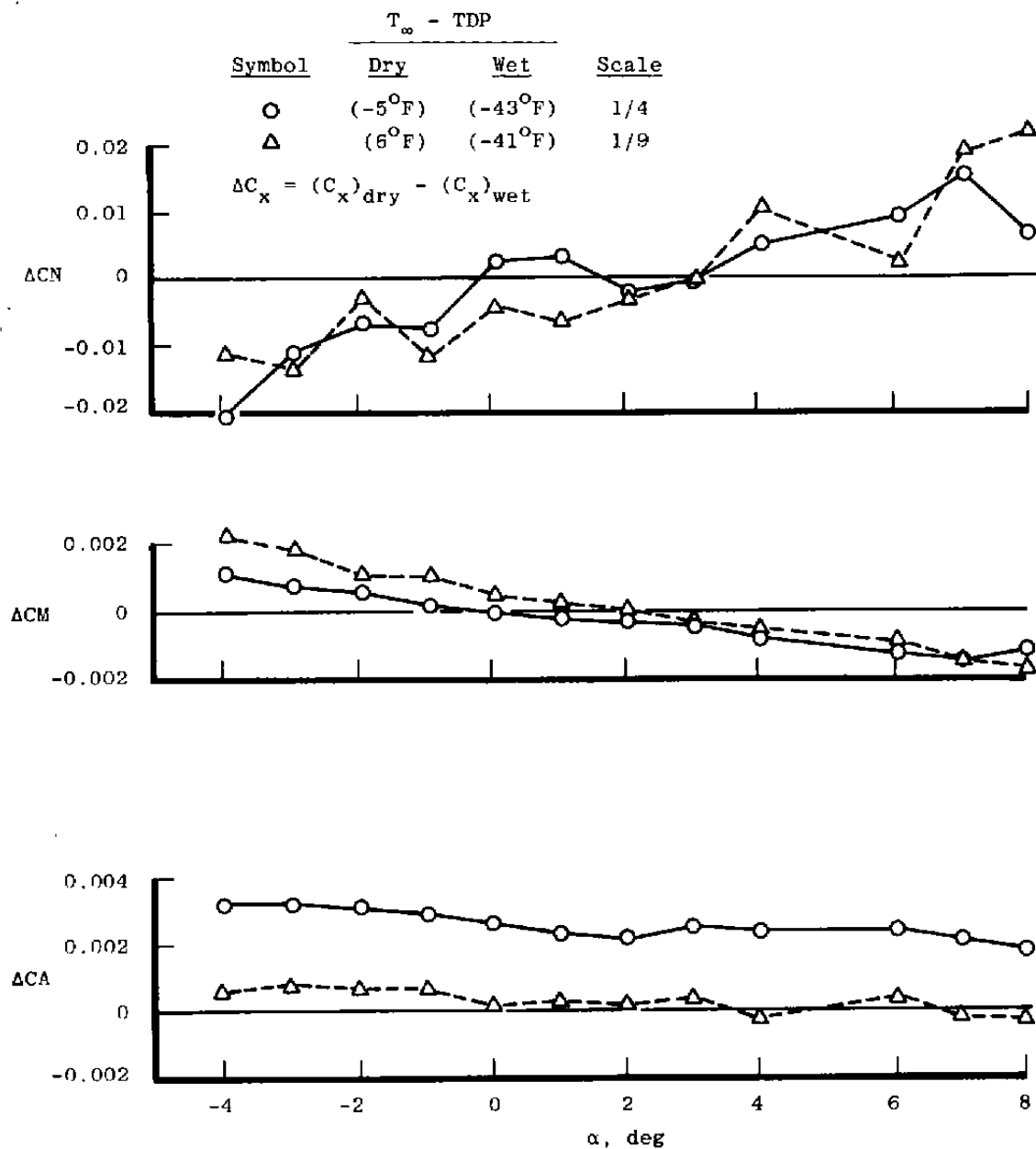Figure 21. Concluded.

Table 1. Test Summary

M_∞	Re $\times 10^{-6}/ft$	Re_L $\times 10^{-6}$	Flow Moisture Content			
			Dry		Vary	Wet
			Model Upright	Model Inverted	Upright	Upright
			1/4-Scale Model			
0.6	2.3	26.6	X	X	---	---
	2.5	28.8	X	---	X	---
0.7	2.2	25.3	X	X	---	---
0.8	2.1	24.2	X	X	---	---
0.9	2.0	23.0	X	X	---	---
	2.5	28.8	X	---	X	X
1.0	1.9	21.9	X	X	---	---
1.1	1.8	20.7	Ⓧ	X	---	---
1.2	1.8	20.7	Ⓧ	X	---	---
	2.5	28.8	X	---	X	X
1.3	1.7	19.6	Ⓧ	---	---	---
1.4	1.6	18.8	Ⓧ	X	---	---
			1/9-Scale Model (Aft Position)			
0.6	2.3	11.8	X	---	---	---
	5.2	26.6	X	X	---	---
0.7	2.2	11.3	X	---	---	---
	4.9	25.3	X	X	---	---
0.8	2.1	10.7	X	---	---	---
	4.7	24.2	X	X	---	---
0.9	2.0	10.2	X	---	---	---
	2.5	12.8	X	---	X	X
	4.5	23.0	X	X	---	---
1.0	1.9	9.7	X	---	---	---
	4.3	22.0	X	X	---	---
1.1	1.8	9.2	Ⓧ	---	---	---
	4.2	21.0	X	X	---	---
1.2	1.8	9.2	Ⓧ	---	---	---
	2.5	12.8	X	---	X	X
	4.0	20.5	X	X	---	---
1.4	1.6	8.2	Ⓧ	---	---	---
	3.6	18.4	X	X	---	---
			1/9-Scale Model (Forward Position)			
0.6	2.3	11.8	X	X	---	---
0.9	2.0	10.2	X	X	---	---
1.2	1.8	9.2	X	X	---	---
1.4	1.6	8.2	X	X	---	---

X – Data acquired at zero wall angle
Ⓞ – Data acquired at optimum wall angle

Table 2. Data Uncertainties

M_∞	Re	UM_i	UC_{P_i}
0.6	2.3	0.003	0.019
	5.1	0.002	0.011
0.7	2.2	0.003	0.017
	4.8	0.002	0.009
0.8	2.1	0.003	0.015
	4.7	0.002	0.008
0.9	2.0	0.003	0.014
	4.5	0.002	0.007
1.0	1.9	0.004	0.014
	4.3	0.002	0.007
1.1	1.8	0.004	0.013
	4.2	0.002	0.006
1.2	1.8	0.004	0.013
	4.0	0.002	0.006
1.3	1.7	0.005	0.013
1.4	3.6	0.006	0.013

NOMENCLATURE

CA	Axial force coefficient
CL	Lift coefficient
CLM	Pitching moment coefficient
CN	Normal force coefficient
C_p	Pressure coefficient, $(P-P_\infty)/Q_\infty$
CP_{BW}	Bottom wall local pressure coefficient
CPN	Pressure coefficient for orifice at Tunnel Station -4
CPN_{avg}	Average pressure coefficient at Tunnel Station -4
CPTW	Top wall local pressure coefficient
CPW	Average of CPTW and CP_{BW}
CPW1-6	Average of CPW for Tunnel Stations 1 through 6
L	Model length, (see Fig. 3)
MN	Average Mach number from Tunnel Station -4 wall pressures
MS	Model station, ft (see Fig. 3)
M_W	Average Mach number for undisturbed orifices in test section, f(CPW)
M_∞	Free-stream Mach number based on tunnel empty calibration
P	Local pressure, psfa
PT	Tunnel stilling chamber pressure, psfa (Fig. 5)
P_∞	Free-stream static pressure, psfa ·
Q_∞	Free-stream dynamic pressure, psfa
Re	Free-stream unit Reynolds number, ft^{-1} per million
Re_L	Characteristic Reynolds (Re X L), per million
Sta,T.S.	Tunnel station relative to front of test section, ft (positive downstream) (see Figs. 1 and 3)

TDP   Dewpoint temperature, °F

T_∞ Free-stream static temperature, °F

U_x Uncertainty in parameter x (Fig. 5 and Table 1)

X/L   Nondimensional model axial distance based on model length (Fig. 3)

α Model angle of attack, deg (positive nose up)

α_f Flow angularity, deg